



Cite this: *Energy Adv.*, 2025,  
4, 1135

## The impact of solvent exposure during preparation on the performance of poly(ethylene oxide)-Li<sub>1.5</sub>Al<sub>0.5</sub>Ge<sub>1.5</sub>(PO<sub>4</sub>)<sub>3</sub> hybrid electrolytes

Gabrielle Foran, \* Cédric Barcha, Caroline St-Antoine, Arnaud Prébé and Mickael Dollé

Hybrid electrolytes are comprised of a salt-containing polymer and an ion-conducting ceramic. The general appeal of these electrolytes is that they combine the desirable properties of each component. Namely, the flexibility, processability and interface compatibility of the polymer and the mechanical strength and high ionic conductivity of the ceramic. In this work, hybrid electrolytes comprised of poly(ethylene oxide) (PEO) and Li<sub>1.5</sub>Al<sub>0.5</sub>Ge<sub>1.5</sub>(PO<sub>4</sub>)<sub>3</sub> (LAGP) were prepared using two different methods: solvent casting in acetonitrile and melt processing using a micro compounder. The presence of added solvents has been shown to impact the properties and stability of polymer electrolytes, but the effect of residual solvents on hybrid electrolytes has not been extensively investigated. Hybrid electrolytes prepared by solvent-free melt processing were compared to those prepared by solution casting, with and without vacuum drying, to determine the impact of solvent exposure on the properties of the electrolyte. Preparation *via* melt processing improved the dispersion of the ceramic phase in the polymer matrix which resulted in lower tortuosity and higher ionic conductivity. The absence of acetonitrile and low water content in the melt-processed sample improved stability during long-term cycling in Li–Li symmetric cells.

Received 24th March 2025,  
Accepted 25th July 2025

DOI: 10.1039/d5ya00082c

[rsc.li/energy-advances](http://rsc.li/energy-advances)

## Introduction

The appeal behind hybrid electrolytes is that they are reported to combine the best properties of polymer and ceramic electrolytes. Namely the high flexibility, processability and interface compatibility of polymer electrolytes with the mechanical strength and high ambient temperature ionic conductivity of ceramic electrolytes.<sup>1,2</sup> Despite this premise, the reported properties of individual hybrid electrolytes, including the ionic conductivity, electrochemical stability and whether or not both phases contribute to ionic conductivity, tend to be variable. These depend heavily on the polymer and ceramic components used to prepare the electrolyte and the proportion of polymer and ceramic in the electrolyte.

For example, Chen *et al.* prepared hybrid electrolytes using PEO (poly(ethylene) oxide)-LiTFSI (lithium bis(trifluoromethane-sulfonyl imide)) and Li<sub>6.4</sub>La<sub>3</sub>Zr<sub>1.4</sub>Ta<sub>0.6</sub>O<sub>12</sub> (LLZTO) where the proportion of ceramic in the electrolyte ranged from 10 to 80 wt%.<sup>2</sup> The highest ionic conductivity was observed at 10 wt% ceramic addition. Ionic conductivity then decreased with increasing LLZTO addition.<sup>2</sup> These findings are likely the result of ionic conductivity

occurring through the polymer phase based on Arrhenius plots provided by the authors which show that the PEO solid polymer electrolyte has the same conductivity mechanism as the hybrid electrolytes.<sup>2</sup> Low levels of ceramic addition can increase the plasticity of the conductive polymer phase whereas increasing ceramic content decreases ionic conductivity due to an increase in tortuosity in the conductive polymer phase.<sup>1,3,4</sup> Although the authors claim the participation of the ceramic phase in the ion conductivity mechanism at higher ceramic loadings,<sup>2</sup> the likelihood of establishing sufficient pressure to obtain a well-connected ceramic particle network within a hybrid electrolyte is unlikely. This effect was demonstrated by Mery *et al.* who compared the ionic conductivities of well-sintered ceramic pellets with those of compacted ceramic powders and PEO-based hybrid electrolytes with different active ceramics.<sup>5</sup> Their results showed that the ionic conductivity of the ceramic pellets that were prepared *via* spark plasma sintering were about three orders of magnitude higher than the ionic conductivities that were measured for compacted ceramic powders.<sup>5</sup> This difference was attributed to grain boundary and charge transfer effects having a greater impact on the ionic conductivity of the loosely-packed sample. The ionic conductivities of PEO-LATP (Li<sub>1.3</sub>Al<sub>0.3</sub>Ti<sub>1.7</sub>(PO<sub>4</sub>)<sub>3</sub>) hybrid electrolytes prepared with 25, 75, and 85 wt% LATP were also analyzed. LATP addition resulted in limited benefits.<sup>5</sup> These results demonstrated that, even

Département de Chimie, Université de Montréal, 1375 Avenue Thérèse-Lavoie-Roux, Montréal, Québec H2V 0B3, Canada. E-mail: gabrielle.foran@umontreal.ca

in samples with high ceramic loading and external pressure, the ionic conductivity of a ceramic pellet is unlikely to be re-created in a hybrid electrolyte.

Although the impact of ceramic loading on the electrochemical performance of hybrid electrolytes has been extensively discussed,<sup>6–9</sup> the impact of the presence of solvents during electrolyte preparation has not. Solution casting, wherein a polymer and salt are dissolved and mixed in a suitable solvent, is a widely used method for the preparation of polymer electrolytes.<sup>10</sup> As hybrid electrolytes are partially comprised of polymer electrolytes, these materials are also often prepared *via* solution casting.<sup>11</sup> It has been known for several decades that the solution casting of PEO-based polymer electrolytes in acetonitrile leaves behind residual solvent as a result of the strong bonds between the solvent and the polymer and the solvent and the ionic salt.<sup>12</sup> More recent studies have shown that residual solvents are very difficult to completely remove from polymer electrolytes despite extensive drying procedures.<sup>13</sup> Exposure to acetonitrile increases the affinity of the lithium cations for the polymer.<sup>14,15</sup> As lithium salts tend to be hygroscopic, water, in addition to acetonitrile is generally absorbed. The presence of water results in a decrease in the glass transition temperature of the polymer and subsequent improvements in ionic conductivity.<sup>16</sup> Although solvent absorption generally results in improved ionic conductivity, the absorption of water and other solvents in hybrid electrolytes tends to be poorly controlled, is not often measured and can negatively impact the long-term stability of the material or battery assembly.<sup>17</sup>

To this end, this work investigates how preparation method, solution casting or dry processing and subsequent sample drying, impact the properties of PEO–Li<sub>1.5</sub>Al<sub>0.5</sub>Ge<sub>1.5</sub>(PO<sub>4</sub>)<sub>3</sub> (LAGP) electrolytes that were prepared with 50 wt% of each component. Electrolyte properties including: the dispersion of the ceramic phase in the polymer matrix, the ionic conductivity of the hybrid electrolyte, the glass transition and melting temperatures of the polymer electrolyte, polymer and lithium ion mobility and the stability of the system during Li–Li cycling will be evaluated. Although the impact of sample preparation and drying procedure have previously been evaluated in polymer electrolytes,<sup>17</sup> similar studies have not been undertaken with hybrid ceramic–polymer electrolytes.

Electrolytes were prepared using two lithium salts, LiTFSI and LiBOB (lithium bis(oxalate)borate). LiTFSI was chosen as it is the most used salt for the preparation of PEO-based polymer electrolytes. LiBOB was selected based on previous research done with liquid electrolytes which shows that the decomposition of the salt can generate a protective layer between the electrolyte and the cathode.<sup>18,19</sup> LiBOB possesses the added advantage of being more environmentally friendly than most other lithium salts. LiBOB decomposes to form non-corrosive, non-fluorinated by-products (B<sub>2</sub>O<sub>3</sub> and CO<sub>2</sub>).<sup>20</sup> This is especially pertinent considering recent government action to ban per- and polyfluoroalkyl substances. LAGP, as opposed to more popular oxide ceramics such as LATP or Li<sub>7</sub>La<sub>3</sub>Zr<sub>2</sub>O<sub>12</sub> (LLZO), was selected for this study due to its higher stability under oxidizing conditions. LLZO is known to react to form La(OH)<sub>3</sub>

upon exposure to humid air under ambient conditions.<sup>21</sup> LATP is considered to be less stable than LAGP with respect to both humid air and lithium metal as the Ti<sup>4+</sup>/Ti<sup>3+</sup> redox reaction occurs more easily than the corresponding reaction with Ge<sup>4+</sup>.<sup>21</sup> Stability in humid air is important for the melt processing part of this study as the micro compounder is located under ambient conditions.

In addition to comparing PEO–LAGP hybrid electrolytes prepared *via* solution casting and melt extrusion, previously published examples of PEO–LAGP hybrid electrolytes (Table 1) will be evaluated to determine whether preparation method has a notable impact on the properties of these electrolytes. This study was limited to systems where the polymer and ceramic components of the electrolyte were mixed. Stacked systems, where polymer–ceramic interactions are forced, were not considered due to differences in the nature of the polymer–ceramic interface and a lack of contact between the ceramic and solvent in the case of electrolyte preparation by solution casting.

Eleven out of the thirteen examples of PEO–LAGP hybrid electrolytes that are presented in Table 1 were prepared using added solvents with acetonitrile being used in eight of these cases. There were two examples of PEO–LAGP that were prepared *via* solvent-free grinding and pressing.<sup>8,9</sup> All of the examples were prepared with LiTFSI, sometimes with another salt, and the relative percentage of LAGP used ranged from 5 to 95 wt% (Table 1). Ionic conductivity was measured in most samples and tended to be on the order of 10<sup>–4</sup> S cm<sup>–1</sup> at 60 °C (Fig. 1) with no glaring differences observed between the samples prepared *via* solution casting and dry pressing. It must be pointed out that although most of the cited authors used precautions such as sample preparation in a dry room or glovebox and drying under vacuum, none of the cited references provided quantitative data on the water and/or residual solvent content of their samples. This makes it difficult to compare the reported conductivity data. Samples prepared without added solvents are not immune to water absorption as both PEO and lithium salts are hygroscopic.<sup>17</sup> This means that the contribution of absorbed water or other solvents to the reported ionic conductivities cannot be discerned.

Ionic conductivities were measured starting at a temperature of 85 or 80 °C and then at descending temperatures until 30 or 25 °C was reached. Most authors performed these measurements in a coin cell configuration. Although absorbed water and residual solvents were not quantified, the similarity in experimental methodology allows these values to be compared. Fig. 1 shows a general trend of higher ionic conductivity in samples that contain less LAGP. This trend is more pronounced at 30 °C where samples that contain 5 wt% ceramic are about two orders of magnitude more conductive than samples that contain more than 80 wt% ceramic (Fig. 1). This trend is present, although less pronounced, at 60 °C where the difference in ionic conductivity between samples that contain low amounts of ceramic and samples that contain high amounts of ceramic is about one order of magnitude (Fig. 1).

The PEO–LAGP samples prepared by Cheng *et al.* and Piana *et al.* were made without added solvents.<sup>8,9</sup> Both of these



Table 1 Previously published examples of PEO–LAGP polymer electrolytes

Salt	Ceramic–polymer ratio	Preparation method	Ref.
LiTFSI	20–60 wt% ceramic	Acetonitrile casting in a dry room	22
LiTFSI	20–60 wt% ceramic	Acetonitrile casting in a dry room	23
LiBF <sub>4</sub>			
LiTFSI	10–80 wt% ceramic	Mixed in mortar without solvent then pressed	8
LiTFSI	10–25 wt% ceramic	Acetonitrile casting	24
LiTFSI	95 wt% ceramic	THF casting in a glovebox, dried at 70 °C	25
LiTFSI	12 wt% ceramic	Acetonitrile casting in a glovebox	6
	14 wt% succinonitrile additive		
LiTFSI	20 wt% ceramic	Acetonitrile casting then sonification and mixing in a Thinky, dried at 50 °C	26
	PEGDA in PEO		
	LAGP aligned by current		
LiTFSI	20–60 wt% ceramic	Room temperature grinding, 80 °C grinding, hot pressing in dry room	9
LiTFSI	26 wt% ceramic	Dissolved polymer in water, LAGP and polymer slurry were poured into an ice template	27
	Contains PEG and PVA		
LiTFSI	50 wt% ceramic	Casting with acetonitrile	28
	Contains 20–40 wt% ionic liquid EMTFSI		
LITFSI	20 wt% ceramic with added melamine	Casting with acetonitrile under vacuum	29
LiTFSI	70 wt% ceramic	Spray painted on to LFP electrode, NMP/IPA solvent	30

samples had relatively high conductivities, especially with higher ceramic loading, at 30 °C. The sample prepared by Piana *et al.* performed similarly at 60 °C: middling conductivity at 20 wt% LAGP with relatively better performance at 40 and 60 wt% LAGP (Fig. 1). This comparison shows that residual solvent from the casting process cannot wholly explain the observed ionic conductivities. In addition to added solvent, ionic conductivity is also impacted by the morphology of the sample. In the case of hybrid electrolytes, this is influenced by the distribution and size of the LAGP particles in the polymer matrix and whether ionic conductivity occurs through the polymer or ceramic phase.<sup>31</sup> If ionic conductivity occurs through the polymer phase, LAGP distribution that reduces tortuosity would result in higher ionic conductivity.<sup>4</sup> If ionic conductivity occurs through the ceramic phase, ionic conductivity would be enhanced by an LAGP particle distribution that results in a percolated ceramic network.<sup>11,25</sup> Cheng *et al.* provide a set of SEM images where the distribution of LAGP in the polymer matrix is compared in samples prepared by cold pressing and those prepared by solution casting.<sup>8</sup> These show that a more uniform distribution of LAGP particles is obtained in the cold pressed sample due to the absence of particle

agglomeration and settling that occur during sample drying when the solution casting method is applied. This is linked to higher ionic conductivity.<sup>8</sup> No morphological information is provided for the samples that were prepared by Piana *et al.*

An analysis of SEM images of hybrid electrolyte cross sections showed that samples that were prepared *via* solution casting but had a secondary means of LAGP particle dispersion *i.e.* applied current (Liu *et al.*<sup>26</sup>) and ice templating (Wang *et al.*<sup>27</sup>) had good LAGP dispersion in the PEO matrix. These samples contained 20 and 26 wt% LAGP respectively. These samples had higher ionic conductivities than the dry pressed samples at both 30 and 60 °C by about an order of magnitude which can be attributed to the dual impact of absorbed solvents and homogeneous LAGP particle distribution. SEM images of cross sections of PEO–LAGP samples prepared by typical solution casting by Wang *et al.* and Lee *et al.* revealed particle agglomeration.<sup>23,25</sup> These samples exhibited some of the lowest ionic conductivities amongst the PEO–LAGP samples compared in Fig. 1. In the case of the electrolyte prepared by Wang *et al.*, this could be attributed to the relatively high ceramic loading (95%) as high loading was also associated with lower ionic conductivity.<sup>25</sup> However, for Lee *et al.*, who prepared samples

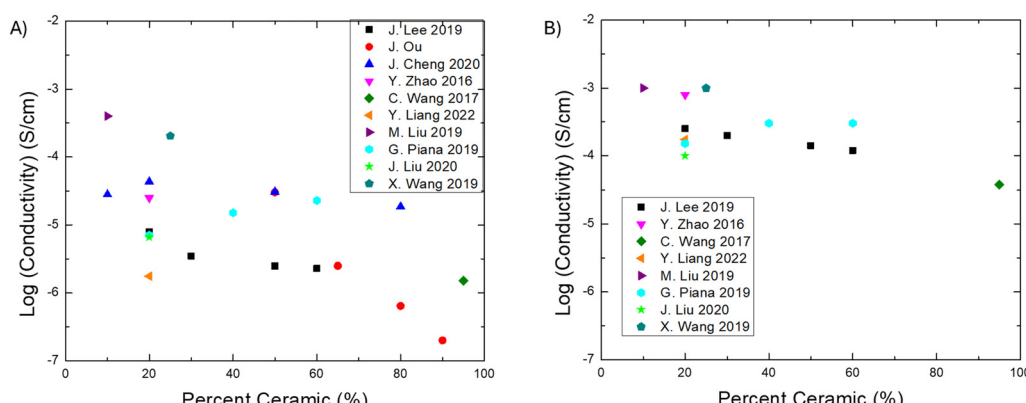


Fig. 1 Ionic conductivity as a function of LAGP content for previously published examples of PEO–LAGP hybrid electrolytes at (A) 30 °C and (B) 60 °C.



with ceramic loadings spanning the 20 to 60 wt% range, the fact that their samples were less conductive than others with similar LAGP loadings suggested that there is a correlation between ceramic particle agglomeration and low ionic conductivity. The other PEO-LAGP samples that are presented in Fig. 1 were either accompanied by inconclusive SEM images (ceramic particles were not observed) or sample imaging was not provided. The above analysis of the relationship between ceramic particle dispersion and ionic conductivity in PEO-LAGP samples prepared by solvent casting and solvent-free preparation methods suggests that uniform particle dispersion has a greater impact on ionic conductivity than the presence of residual solvents. This interpretation is however limited as information on water/solvent content was not provided for any of the referenced systems.

One polarizing issue that concerns hybrid electrolytes is whether the presence of two ion-conducting phases provides any real advantage in terms of ionic conductivity. Amongst the publications presented in Table 1, four provided a comparison between their hybrid electrolytes and a PEO solid polymer electrolyte. Lee *et al.* showed that their hybrid electrolytes with 20 and 30 wt% LAGP loading were more conductive than the PEO-LiTFSI electrolyte below 60 °C whereas their electrolytes with higher ceramic loading were less conductive at all temperatures.<sup>22</sup> The observed trend of hybrid electrolytes with lower LAGP loadings being more conductive than PEO-based solid polymer electrolytes was also present in the work of Liu *et al.* and Zhao *et al.* whose hybrid electrolytes with 12 and 20 wt% LAGP respectively were more conductive than their PEO solid polymer electrolyte analogues.<sup>6,24</sup> All electrolytes presented a conductivity curve that is characteristic of PEO-LiTFSI wherein a break in the slope corresponding to the  $T_m$  of PEO-LiTFSI is observed. This thermal transition has been reported to occur at 55 °C for a sample containing 23 wt% LiTFSI which is close to the value used in the cited publications.<sup>32</sup> The presence of a break in slope near the melting point of PEO-LiTFSI suggests that ionic conductivity in these samples occurs through the PEO phase only. It is unlikely that a sufficiently connected ceramic network, which is necessary for long-range ion transport, has been established at low ceramic loadings.<sup>5</sup> The slight increase in conductivity observed at low ceramic loading could be attributed to a further disruption of PEO crystallinity by the ceramic particles.<sup>6</sup> Higher LAGP loading is likely correlated with lower ionic conductivities due to increased tortuosity in the conductive PEO phase.<sup>33</sup>

Contradicting evidence was provided by Piana *et al.* who showed improved ionic conductivity with increasing ceramic loading below 60 °C. Ionic conductivities at 60 °C were similar for the PEO-LiTFSI sample and the hybrid electrolytes that contained 40 and 60 wt% LAGP.<sup>9</sup> The sample with 20 wt% LAGP had the lowest ionic conductivity. A change in slope between 50 and 60 °C was observed on the graph of conductivity as a function of temperature suggesting that ionic conductivity still occurs in the PEO phase in these samples. The major difference between these samples and the ones discussed above is that they were prepared *via* a solvent-free hot-pressing process as

opposed to solution casting. It is therefore possible that the absence of absorbed solvents, and the subsequent decrease in polymer plasticization,<sup>34</sup> resulted in overall lower polymer chain mobility in the samples prepared by Piana *et al.*<sup>9</sup> Reduced plasticization could enhance the impact of the addition of ceramic particles on the degree of polymer crystallinity.

The possibility of the participation of both the ceramic and polymer phases in ion conduction was discussed by Ou *et al.* Analysis of their Nyquist plots revealed both a high frequency element that was attributed to ionic conductivity through bulk LAGP and a lower frequency element that was attributed to ionic conductivity through both the LAGP grain boundary and PEO-LiTFSI which could not be separated.<sup>28</sup> These findings suggest that both the ceramic and polymer phases participate in the observed ionic conductivity. The authors then added an ionic liquid which increased the conductivity of the polymer phase. Conductivity was then observed to occur through the polymer phase only. These findings are consistent with observations made by Isaac *et al.* which show that ionic conductivity tends to occur through the more conductive phase in organic/inorganic electrolyte systems.<sup>4</sup> Ionic conductivity through both polymer and ceramic domains is claimed but interfacial behaviour or the possibility of chemical exchange of lithium ions between these domains is not discussed in the proposed conduction mechanisms.<sup>28</sup>

A more detailed discussion of ionic conduction mechanism in an electrolyte prepared *via* casting in acetonitrile is provided by Liu *et al.*<sup>6</sup> They attribute improved conductivity in the hybrid electrolyte to participation of both the polymer and ceramic phases in the observed ionic conductivity. The measurement of  ${}^7\text{Li}$   $T_1$  (spin lattice) relaxation indicated the presence of two motional processes: one short range and one long range.<sup>6</sup> A  ${}^6\text{Li}$  labeling experiment where the hybrid electrolyte was cycled with  ${}^6\text{Li}$  lithium metal electrodes showed an increase in the proportion of  ${}^6\text{Li}$  in the LAGP phase following cycling in addition to the formation of a new lithiated environment that occurred only in the presence of LAGP. The authors propose that this evidence indicates the formation of a polymer-ceramic interface which participates in ionic conduction along with the polymer and ceramic phases.<sup>6</sup> Although an interaction with the LAGP phase and the formation of an interface during cycling are supported by the data provided by the authors, the lack of mechanistic difference between ionic conductivity in the polymer and hybrid electrolytes suggests that the participation of the ceramic phase may be limited to the local scale (short-range motional process) with ion conduction by polymer chain mobility playing the biggest role in long-range ion transport.

Liu *et al.* also claimed to have observed the participation of the ceramic phase in PEO-LAGP electrolytes that were doped with succinonitrile.<sup>6</sup>  ${}^6\text{Li}$  NMR following cycling with  ${}^6\text{Li}$  enriched lithium foils showed  ${}^6\text{Li}$  in the LAGP phase and the formation of an interface between the polymer and ceramic phases. It is proposed that the interface permits the chemical exchange of lithium between the polymer and ceramic phases.<sup>6</sup> The spectroscopic analysis of comparable PEO-LiTFSI and PEO-LAGP-LiTFSI electrolytes without added succinonitrile is



not presented in this work making it difficult to conclude whether the interface that forms upon cycling is the result of an interaction between the solvent and the ceramic that causes it to interact with the  ${}^6\text{Li}$ . Liu *et al.* who prepared electrolytes with both randomly dispersed and aligned LAGP particles state that ion conduction can occur through the ceramic particles in the aligned systems.<sup>26</sup> The observed higher ionic conductivity in the aligned systems (half an order of magnitude) was attributed to this morphology. However, Nyquist plots presented by the authors for both materials indicate that ionic conductivity occurs through a single phase.<sup>26</sup> The change in slope observed in the conductivity curve around the melting point of PEO suggests that the observed ionic conductivity occurs through the polymer phase alone. The observed increase in ionic conductivity in the aligned sample could instead be the result of differences in tortuosity caused by LAGP particle distribution within the polymer matrix.

Piana *et al.* provided an analysis of the role of the LAGP and PEO phases in the ionic conductivity of a hybrid electrolyte prepared *via* hot pressing in the absence of solvents.<sup>9</sup> An analysis of the ionic conductivity and lithium transport numbers (as determined by electrochemical methods) leads to the conclusion that ionic conductivity occurs exclusively through the PEO phase at 60 °C and above when the  $T_m$  has been surpassed and the polymer is most mobile. The fact that increasing LiTFSI content did not lead to a significant change in lithium transport number resulted in the conclusion that LAGP plays a role in lithium ion conduction at lower temperatures.<sup>9</sup> An analysis of their conductivity data shows that conductivity plots for all of the hybrid samples exhibit the same general shape as that of the PEO-LiTFSI electrolyte despite having higher ionic conductivities below 60 °C. This could be attributed to changes in polymer chain mobility due to the presence of LAGP as opposed to the participation of LAGP in ion conductivity.

PEO-LAGP electrolytes were cycled by various authors in Li-Li, Li-LFP (lithium iron phosphate) and, in the case of Liang *et al.*, Li-NMC (lithium nickel manganese cobalt oxide) cells (Table 2).<sup>6,8,9,24,27–30</sup> All cycling in LFP- and NMC-based systems was done using electrodes that were prepared *via* solution casting that did not contain LAGP. This was even the case for the electrolytes that were made by Piana *et al.* and Cheng *et al.* which were produced *via* hot pressing.<sup>8,9</sup> The possibility of absorbed solvents in the electrodes and possible effects on cell stability can therefore not be discounted. Attempts at cycling hybrid systems with electrodes prepared *via* solvent-free processing techniques and/or electrodes that contain LAGP have yet to be published. A direct comparison of the referenced systems is difficult to perform due to the extensive variability in cycling conditions used by the authors.<sup>35</sup>

Li-Li cells were compared by determining the capacity of the cell based on the charge density and the number of hours that the system was cycled for. Although it is unknown whether these systems were analyzed to failure, the reported calculated capacities can be compared. The highest capacity, 325 mAh cm<sup>-2</sup> was reported by Liang *et al.* in a solvent-casted system that contains 20 wt% LAGP. The system also contained melamine

**Table 2** Cycling parameters for Li-Li, Li-LFP and Li-NMC cells with PEO-LAGP electrolytes

Temperature (°C)	Time (h)	Current density (mA cm <sup>-2</sup> )	Capacity (mAh cm <sup>-2</sup> )	Ref.
Li-Li cells				
50 <sup>a</sup>	<b>1500</b>	<b>0.05</b>	75	8
25	800	0.05	40	6
<b>60</b>	<b>100</b>	<b>0.2</b>	20	9
60	200	0.1	20	27
60	1300	0.25	325	29
Li-LFP cells				
<b>50</b>	<b>100</b>	<b>0.1</b>	136	8
60	50	0.1	166	24
25	10	0.05	120	6
<b>80</b>	<b>10</b>	<b>0.1</b>	<b>140</b>	9
60	300	0.3	150	27
50	120	0.3	82.5	28
60	180	0.3	133	29
60	100	0.1	151	30
Li-NMC523 cells				
60	125	0.2	86	29

<sup>a</sup> Values in bold indicate PEO-LAGP prepared without solvents.

that was mixed with the LAGP prior to solution casting. The best performing solvent-free system was a 20 wt% LAGP electrolyte prepared by Cheng *et al.* with a capacity of 75 mAh g<sup>-1</sup>. These results suggest better overall performance and stability in systems prepared *via* solution casting (Table 2). Although the authors do not report the possibility of the impact of residual acetonitrile, the demonstrated long-term stability in Li-Li cells implies that the electrolyte has either been sufficiently dried or that the solvent is not overly reactive with respect to lithium metal. The evolution of the electrolyte–lithium metal interface would need to be studied over time to confirm these hypotheses. Cycling in Li-LFP and Li-NMC cells also showed that the solution-casted electrolytes outperformed their solvent-free counterparts as higher capacities were generally attained at faster cycling rates for longer durations (Table 2). Cheng *et al.* compared their cold-pressed electrolytes to solution casted electrolytes.<sup>8</sup> Although the cold-pressed electrolytes demonstrated better ionic conductivity and LAGP dispersion than their solution-casted counterparts, Li-Li and Li-LFP cells were not prepared using the cold-pressed electrolytes.

The above evaluation of ionic conductivity, lithium exchange between the polymer and ceramic phases and stability during cycling in previously published PEO-LAGP hybrid electrolyte systems reveals important themes. There is a general trend of ceramic loading above 20 wt% resulting in lower ionic conductivity than when ceramic loading is between 5 and 20 wt% (Fig. 1). Additionally, the probable presence of water and casting solvent does not seem to enhance polymer mobility. Although polymer mobility and solvent content were not quantified by most authors, the hybrid electrolytes that were prepared by solution casting did not significantly outperform those that were prepared by hot pressing as would be expected



based on differences in ionic conductivity in polymer electrolytes that contain absorbed solvent.<sup>17,34</sup> These findings suggest that ceramic dispersion, which is poorer in samples prepared by solution casting, also contributes to the reported ionic conductivities. These factors will be addressed here by preparing a series of PEO-LAGP samples *via* solution casting and solvent-free methods wherein properties such as water content, acetonitrile content and ceramic dispersion will be evaluated to determine their impact on the thermal properties, ionic conductivity, ion and polymer mobility and stability with respect to lithium metal. Samples will be prepared with 50 wt% ceramic loading such that ceramic particle agglomeration, if present, would have a significant impact on ionic conductivity. Additionally, increasing the volumetric fraction of the ceramic phase provides an opportunity for ion conduction through the ceramic phase and/or lithium exchange between phases to be observed.

## Experimental

### Electrolyte preparation

The solution-casted (SC) electrolytes were prepared by completely dissolving PEO (5 000 000 M, Sigma Aldrich) in acetonitrile. 24.5 wt% LiTFSI with respect to the weight of the polymer was dissolved into the solution. For samples prepared with LiBOB (lithium bis(oxalato)borate), the weight of the salt was determined such that the number of moles of lithium was equal to the number of moles of lithium in the sample prepared with LiTFSI. An equivalent weight of LAGP powder (300–500 nm, MSE Supplies) was added to the dissolved polymer electrolyte. The mixture was stirred overnight, sonicated for two hours and then poured out into a glass dish. The sample was left overnight in the fume hood to evaporate the acetonitrile. All stirring and evaporation steps were performed at room temperature. The resultant film was hot pressed (130 °C) before being further dried: first overnight in a vacuum oven at 60 °C, then overnight under active vacuum in a glovebox port that was heated to 60 °C. Sample water content was determined using a Computrac Vapor Pro XL (Arizona). The sample prepared with LiTFSI contained 2100 ± 100 ppm water. The sample prepared with LiBOB contained 3400 ± 100 ppm water. Undried solution-casted (WET) PEO-LAGP samples were prepared as described above except that both vacuum drying steps were omitted. The purpose of the WET solution-casted samples was to provide a point of comparison with the melt-processed samples that contain the most water and/or acetonitrile possible. Sample water content was quantified using the Computrac Vapor Pro XL. The LiBOB-containing sample had an average water content of 30 900 ± 900 ppm. The LiTFSI-containing sample had an average water content of 46 000 ± 3000 ppm. These values surpass those of as-prepared electrolytes made by Mankovsky *et al.*, falling within the range of PEO-based electrolytes that were doped with additional water following drying.<sup>17</sup> The water content in the SC and WET samples is partially dependent on the distribution of LAGP.

Ceramic particle agglomeration during the casting and evaporation steps were shown to result in uneven distribution of LAGP in PEO relative to the samples that were prepared *via* melt processing. PEO and LAGP have different levels of hygroscopicity. It is therefore assumed that the differences in water content between the LiBOB and LiTFSI samples that were prepared *via* the SC and WET methodologies are the result of ceramic distribution and not related to the presence of LiTFSI or LiBOB salts. The water content of the LiTFSI- and LiBOB-containing samples are the same within error following preparation by MP (melt-processed) and ACE methods where an even distribution of ceramic is observed.

The MP samples were prepared *via* solvent-free melt extrusion using an Xplore MC 15 HT micro compounder. Equivalent weights of PEO (5 000 000 M, Sigma Aldrich) and LAGP powder (300–500 nm, MSE Supplies), along with lithium salt were added to the micro compounder in alternation. The mass of LiTFSI used was 24.5% of the mass of PEO. The mass of LiBOB was selected such that samples prepared with LiBOB contained the same number of moles of lithium as samples prepared with LiTFSI. The mixture was processed for 15 minutes at 110 °C with a screw speed of 50 rpm. Samples were pressed into films at 130 °C using a hot press. The resultant films were dried overnight under active vacuum in a glovebox port at 60 °C. A Computrac Vapor Pro XL (Arizona) was used to measure sample water content. The sample prepared with LiTFSI contained 3600 ± 400 ppm water. The sample prepared with LiBOB contained 4000 ± 800 ppm water. ACE samples were prepared similarly except that the LAGP particles were soaked in acetonitrile for one day. The acetonitrile was then evaporated in the fume hood. The resultant powder was dried overnight under vacuum at 60 °C prior to being used to produce hybrid electrolytes by melt processing as described above. These samples contained 3600 ± 300 ppm and 3500 ± 400 ppm water with LiTFSI and LiBOB salts respectively. The ACE samples were prepared to compare this system to the simulated PEO-LATP interfaces prepared by Mangani *et al.* where immersion of the ceramic surface in acetonitrile for one minute followed by subsequent drying was found to decrease resistance at the ceramic-polymer interface.<sup>36</sup> It was additionally of interest to determine whether soaking the ceramic particles in acetonitrile impacted their dispersion in the PEO polymer matrix.

### Differential scanning calorimetry (DSC)

DSC measurements were performed using a PerkinElmer DSC6000. Samples were heated between –70 and 150 °C at a rate of 10 °C min<sup>–1</sup> then cooled to –70 °C at the same rate. These steps were followed by a second heating step (–70 to 150 °C at 10 °C min<sup>–1</sup>) from which the thermal data was extracted. An additional program wherein the sample was heated between –50 and 220 °C at a rate of 10 °C min<sup>–1</sup> was used to characterize the WET PEO(LiBOB)-LAGP, boric acid and oxalic acid samples.

### Scanning electron microscopy/energy dispersive X-ray spectroscopy (SEM/EDX)

Samples were chilled using dry ice prior to being sliced in half using a razor blade. A field emission gun-scanning electron



microscope (Quattro) operated at 5 kV and low current was used to acquire images of the sample. A Thermo Fisher Phenom XL G2 desktop SEM instrument operated at 10 kV and low current was also used. Samples were coated with a thin layer of gold ( $\sim 10$  nm) prior to analysis to avoid static electric charges and surface deterioration. Energy dispersive X-ray spectroscopy (EDX) was performed to evaluate sample composition.

### Electrochemical impedance spectroscopy

Ionic conductivities were measured in 10-degree increments between 30 and 80 °C using a Biologic SP-300 with frequencies between 7 MHz and 100 mHz and an amplitude of 10 mV. The electrolytes were sealed in coin cells inside of a glovebox for all conductivity measurements. The sample was first heated to 80 °C with subsequent measurements being performed at decreasing temperatures. The sample temperature was equilibrated for two hours prior to acquiring measurements.

### Lithium–lithium cycling

Lithium–lithium symmetric cells were prepared using the hybrid electrolytes made *via* the wet and dry processing methods that are detailed above. Hybrid electrolytes were calendered to a thickness of 30–45  $\mu\text{m}$  using a Collin laboratory calendering machine. A thin PEO layer (30–45  $\mu\text{m}$ ) was adhered to a sheet of lithium metal (40  $\mu\text{m}$  Li on 11  $\mu\text{m}$  copper, MSE Supplies) using a credit card laminator inside a glovebox. A 16 mm punch of calendered hybrid electrolyte was placed between two sheets of PEO-coated lithium metal. The resultant stack was laminated together and sealed inside a coin cell. Li–Li cycling was performed at a current density of 0.05 mA  $\text{cm}^{-2}$  at 60 °C using a BioLogic VMP2. Fifty charge/discharge cycles lasting 30 minutes were performed prior to acquiring impedance spectra. The series was repeated six times resulting in a total of 325 hours of cycling yielding a capacity of 16 mAh  $\text{cm}^{-2}$ . Cycling in lithium–lithium cells was repeated until two runs showing similar tendencies were obtained.

### Nuclear magnetic resonance (NMR) spectroscopy

Samples were packed into 4 mm rotors inside the glovebox. One dimensional  $^1\text{H}$ ,  $^7\text{Li}$  and  $^{19}\text{F}$  spectra were acquired using a 9.4 T Bruker Avance spectrometer equipped with a 4 mm double resonance MAS (magic angle spinning) probe.  $\pi/2$  pulse lengths of 4.1  $\mu\text{s}$ , 5.4  $\mu\text{s}$  and 6  $\mu\text{s}$  were calibrated at power levels of  $-18.30$  dB,  $-22.3$  dB and  $-15.90$  dB for  $^1\text{H}$ ,  $^7\text{Li}$  and  $^{19}\text{F}$  respectively.  $T_1$  (spin-lattice) relaxation was measured using an inversion-recovery pulse sequence. Pulsed field gradient (PFG) NMR was used to measure diffusion coefficients for all three nuclei. Gradients pulses lasting 5 ms were applied for diffusion times ranging from 600 to 2000 ms. Total gradient strength was 50. All experiments were performed at a MAS-calibrated 60 °C.  $T_1$  relaxation times and  $^{19}\text{F}$  diffusion coefficients were collected from a single measurement due to the low degree of uncertainty. The  $^1\text{H}$  diffusion coefficients and  $^7\text{Li}$  diffusion coefficients are the average of three runs. The lower diffusion rates of the lithium ions and the PEO polymer

backbone results in them being more difficult to capture with the available equipment, thereby increasing the error associated with these measurements.

### Infrared (IR) spectroscopy

Infrared spectra were measured outside the glove box using a Tensor Fourier Transform Infrared spectrometer from Bruker Optics in attenuated total reflection mode with a silicon crystal (MIRacle, Pike Technologies). The acquired spectra were an average of 100 scans with a 4  $\text{cm}^{-1}$  resolution and 8 degrees zero filling. Data were collected from two separate samples over a range of 4000 to 500  $\text{cm}^{-1}$ .

## Results and discussion

Data presented in Fig. 1 and Table 2 show that PEO–LAGP hybrid electrolytes prepared *via* solvent-free methods demonstrate no significant advantages over similar electrolytes that were prepared *via* solution casting in terms of electrochemical performance. Solvent-free preparation methods were shown to result in better ceramic dispersion in the polymer matrix but this can be compensated by templating or otherwise aligning the ceramic particles in solution-casted electrolytes.<sup>8,26</sup> Despite these findings, it is difficult to compare samples that were prepared and evaluated under different conditions. For this reason, PEO–LAGP samples were prepared *via* both solution casting and solvent-free melt processing are investigated in this work. Additional solution-casted samples that were not dried under vacuum and melt processed samples where the LAGP was pre-soaked in acetonitrile were prepared to better evaluate the role of absorbed water and residual solvents in electrolyte performance. These samples were evaluated under the same set of experimental conditions to facilitate comparison. Samples were made using either LiTFSI or LiBOB to gauge how the salt anion impacts the properties of these hybrid electrolytes. LiTFSI was chosen as it is one of the most used salts in polymer electrolytes. LiBOB was chosen because it does not contain fluorine, making it a material of interest considering upcoming bans on fluorinated materials in several countries.

One significant difference between the solution casting and melt processing preparation methods used in this work is the amount of time and resources that were required to produce an electrolyte with each method. The melt-processed samples were prepared by directly mixing lithium salt and LAGP powder into molten PEO. Samples were prepared at 110 °C and mixed for a total of 15 minutes to ensure homogeneity. Preparation *via* solution casting required PEO and lithium salt to be dissolved in acetonitrile (roughly 250 ml/5 g polymer). The dissolution process was completed overnight prior to the addition of LAGP. LAGP was dispersed in the dissolved PEO by a combination of stirring and sonication. The mixed solution was then poured out and left to dry for 24 hours in a fume hood to evaporate the acetonitrile. Both melt-processed and solution-casted samples were pressed and calendered to obtain the final electrolyte thicknesses used in this work. The melt processed samples



were easier to shape *via* calendering than the solution-casted samples. The SC samples were dried twice overnight under vacuum whereas the MP samples were dried under vacuum once. The WET solution casted samples were not dried aside from solvent evaporation in the fume hood. The additional dissolution and drying steps resulted in the preparation of the solution-casted samples being more time consuming. Even the WET samples, which were not dried under vacuum, took longer to prepare than the MP samples due to long polymer dissolution and homogenization times. Additional costs associated with the use of acetonitrile and energy associated with solvent evaporation are expected to become significant in the large-scale production of polymer electrolytes. In addition to the longer drying and mixing times, the sedimentation and agglomeration of LAGP particles during preparation *via* solution casting had significant consequences on the morphology of the prepared samples.

Ceramic particle distribution in the polymer matrix differed significantly between hybrid electrolytes prepared *via* solution casting and solvent-free methods. This is of significant importance as the characteristics of the composite electrolyte depend on the homogeneity of the LAGP dispersion in the PEO matrix.<sup>37</sup> Due to the need for solvent evaporation, solution-casted hybrid electrolytes are known to experience ceramic particle agglomeration.<sup>8</sup> This was investigated by performing SEM imaging of the MP and SC PEO-LAGP samples. Fig. 2 shows cross sections of the hybrid electrolyte samples. Fig. 2A and B, which depict the samples that were prepared by melt processing, show uniform dispersion of the LAGP phase, as determined by the EDX mapping of germanium. More particle agglomeration was observed in the SC and WET samples than in the MP and ACE samples (Fig. 2 and Fig. S1). The absence of particle agglomeration in the ACE samples shows that particle distribution is more dependent on preparation method (solution casting or melt processing) than on the presence of solvents in the sample. The use of LiTFSI or LiBOB did not appear to impact LAGP particle dispersion in the hybrid electrolytes. It is anticipated that particle dispersion could influence sample properties such as polymer chain crystallinity and mobility. These will be evaluated using DSC, NMR spectroscopy and EIS.

DSC was performed to determine whether exposure to acetonitrile and/or LAGP particle dispersion impacts the thermal properties of these electrolytes. Melting temperature ( $T_m$ ) and glass transition temperature ( $T_g$ ) of the PEO phase are reported in Fig. 3. The impact of the lithium salt anion, TFSI<sup>-</sup> or BOB<sup>-</sup>, on polymer chain mobility was also evaluated. The data presented in Fig. 3 represent the average of two runs.

PEO  $T_g$  was similar within error for all PEO-LAGP samples, indicating that preparation method and salt anion did not significantly influence this parameter (Fig. 3). Although absorbed water and other solvents are supposed to act as plasticizers and lower the  $T_g$  of polymer samples,<sup>38</sup> the average glass transition temperatures of the WET samples were only marginally lower than those of the MP, ACE and SC samples despite the fact that they contained around ten times as much water (in ppm). The SC, ACE and WET samples were exposed to

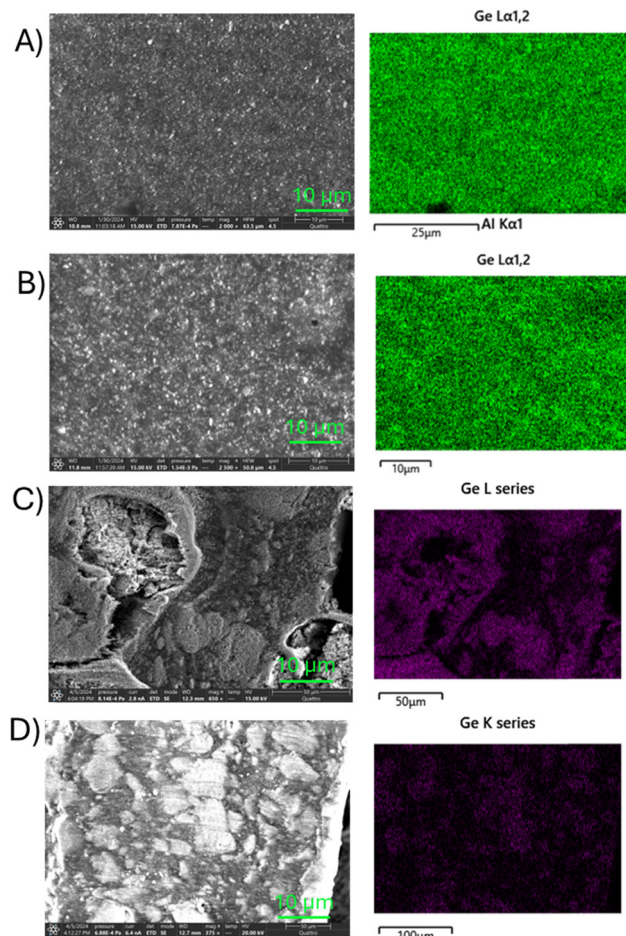


Fig. 2 SEM images of sliced PEO-LAGP electrolytes with germanium mapping via EDX. (A) PEO(LiTFSI)-LAGP MP, (B) PEO(LiBOB)-LAGP MP, (C) PEO(LiTFSI)-LAGP SC, (D) PEO(LiBOB)-LAGP SC. All images represent cross sections of the hybrid electrolytes. Samples were sliced with a blade following cooling with dry ice. The images were acquired with an accelerating voltage of 15 kV and magnifications ranging from 670 to 2300 $\times$ .

acetonitrile during sample preparation. Acetonitrile interacts differently with PEO than water does. Hakem *et al.* found that absorbed acetonitrile coordinates to ether oxygen groups on the polymer backbone and decreases polymer chain mobility whereas water hydrogen bonds to PEO, reducing its interaction with lithium ions, thereby increasing ion mobility.<sup>14</sup> Trace amounts of acetonitrile are therefore not expected to lower  $T_g$ .

Average  $T_m$  for PEO was highest in the SC samples and lowest in the MP samples (Fig. 3). This finding was unexpected as absorbed solvents are generally expected to act as plasticizers in PEO-based electrolytes.<sup>34</sup> This is however correlated with sample water content measurements which show that the SC samples contain the least water. The presence of fillers is also generally thought to result in decreased crystallinity in PEO.<sup>39</sup> This effect can be directly observed in the MP samples whose  $T_m$  values are significantly lower than those of PEO(LiBOB) and PEO(LiTFSI) samples that were prepared *via* melt processing,  $56.4 \pm 0.3$  and  $58.7 \pm 0.4$  °C respectively. The observed modest decrease in  $T_m$  correlates with work presented by Lee *et al.* who



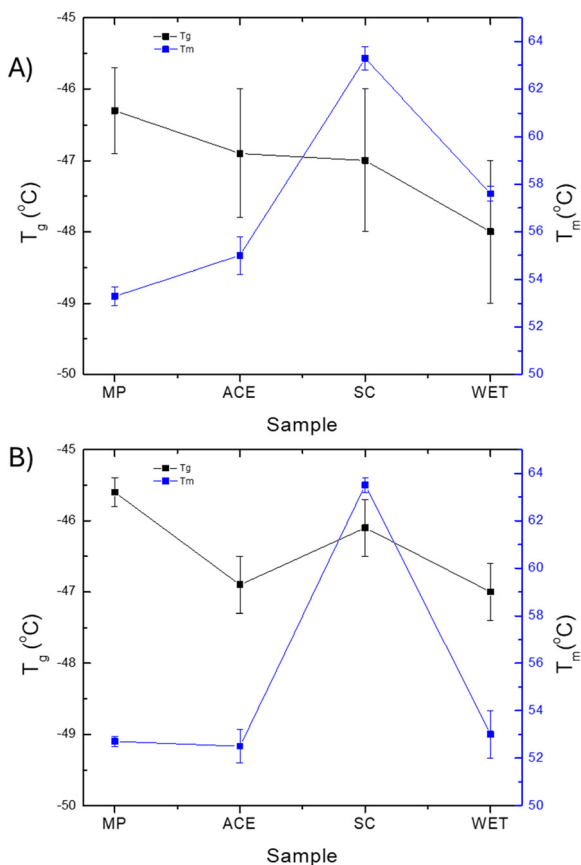


Fig. 3  $T_g$  and  $T_m$  of PEO(LiTFSI)-LAGP (A) and PEO(LiBOB)-LAGP (B) as determined by DSC. Samples were heated from  $-50$  to  $150$  °C at a rate of  $10$  °C min $^{-1}$  during data collection.

observed an approximately 3 °C decrease in  $T_m$  in PEO(LiTFSI) with the addition of 50 wt% LAGP.<sup>23</sup> The observation of the lowest  $T_m$  in the MP samples is likely the result of the homogeneous distribution of LAGP in these samples (Fig. 2). The impact of fillers on polymer chain crystallinity is expected to be greater when said fillers are well-dispersed amongst the polymer chains. The decreased  $T_m$  in the WET samples relative to the SC samples is expected to be the result of increased water content as both samples were found to exhibit LAGP particle agglomeration (Fig. S1). The limited difference in  $T_m$  between the hybrid electrolytes relative to PEO(LiTFSI) and PEO(LiBOB) solid polymer electrolytes is thought to result from weak interactions between PEO and LAGP, giving LAGP a limited influence on the thermal properties of the polymer.<sup>23</sup>

The WET PEO(LiBOB)-LAGP sample exhibited three additional thermal transitions that were not observed in any of the other samples: a  $T_g$  at 157 °C and  $T_m$  peaks at 171 and 189 °C (Fig. S2). These were attributed to the  $T_g$  and  $T_m$  of boric acid and the melting of oxalic acid respectively.<sup>40,41</sup> Bis(oxalato)-borate is known to decompose to yield boric and oxalic acids.<sup>42</sup> The process can occur in the presence of both water and acetonitrile making it most likely to occur in the WET PEO(LiBOB)-LAGP sample. The observation of additional phases via DSC was correlated with the appearance of crystalline

structures in the PEO(LiBOB)-LAGP WET but not the other PEO(LiBOB)-LAGP samples as observed by SEM (Fig. S3). The presence of boric acid, oxalic acid and residual acetonitrile were verified *via* infrared and NMR spectroscopies.

Infrared spectroscopy was performed to verify the presence of acetonitrile in the SC, ACE and WET samples and to determine whether the decomposition of LiBOB resulted in the formation of boric and oxalic acid in the LiBOB-containing WET hybrid electrolytes as is suggested by DSC (Fig. S2). IR spectra of the PEO(LiTFSI)-LAGP samples show that there are no significant differences between these samples (Fig. S4). Two spectra of each material were collected and no evidence of acetonitrile was found for the SC, ACE and WET samples despite exposure to the solvent during sample preparation. The IR results indicate that drying overnight in a fume hood resulted in most of the acetonitrile being evaporated from the hybrid electrolyte. Some differences that correlate with the decomposition of LiBOB were observed in the PEO(LiBOB)-LAGP spectra. Notably, a peak at  $1803$  cm $^{-1}$ , attributed to the carbonyl stretching vibration in free LiBOB was absent from the spectrum of the WET sample (Fig. S4).<sup>43</sup> This was correlated with the appearance of a peak at  $1743$  cm $^{-1}$  which corresponds to the carbonyl stretching vibration in crystalline oxalic acid in the SC, ACE and WET samples (Fig. S4).<sup>44</sup> An additional peak at  $1327$  cm $^{-1}$  was observed in the spectrum of the WET sample only (Fig. S4). This was assigned to the OH bending vibration of oxalic acid.<sup>44</sup> Peaks corresponding to boric acid were not observed by IR spectroscopy as the B–O and O–H vibrations overlap with those that are expected for LiBOB and PEO respectively.

The presence of these species was also investigated using proton NMR spectroscopy.  $^1\text{H}$  NMR (Fig. S5) showed that trace amounts of acetonitrile were present in the WET samples but not the SC or the ACE samples. This finding demonstrates that the additional vacuum drying steps contributed to the elimination of this solvent whereas drying in the fume hood only was not sufficient. As for boric and oxalic acids which could be observed *via* DSC, a peak at 5.47 ppm corresponding to boric acid was observed in PEO(LiBOB)-LAGP WET only (Fig. S4). This indicates that the presence of increased quantities of water and acetonitrile in the WET sample resulted in the decomposition of LiBOB. This phenomenon was not observed in the MP, ACE or SC samples due to less water and acetonitrile being present. Amereller *et al.* who studied the impact of temperature and water content on the hydrolysis of LiBOB, found that several weight percent water were needed to produce observable decomposition at 25 °C.<sup>42</sup> LiBOB decomposition was found to occur more readily at 60 °C,<sup>42</sup> which would explain the increased visibility of the LiBOB degradation products by DSC. Peaks corresponding to oxalic acid, expected around 11 ppm, were not observed. These findings show that the presence of absorbed solvents can impact the stability of the lithium salt. Although these effects were only observed in the WET samples, the impact of differences in electrolyte stability on polymer and salt mobility, ionic conductivity and stability with respect to lithium metal electrodes will be investigated in the following sections.



Polymer chain mobility was evaluated using  $^1\text{H}$   $T_1$  relaxation times and proton diffusion coefficients to determine whether preparation method had a significant impact on polymer chain mobility and consequently on ionic conductivity. Preparation method had some impact on  $^1\text{H}$   $T_1$  relaxation time. The slowest proton relaxation times, indicative of lower polymer chain mobility, were observed for the MP samples (Fig. 4). This correlates with low water content and the absence of absorbed solvents generally resulting in lower polymer chain mobility.<sup>34</sup> The fastest  $T_1$  relaxation was observed in the WET samples (Fig. 4) where water content was by far the highest. Samples prepared with LiTFSI tended to have faster  $^1\text{H}$  relaxation than samples prepared with LiBOB. This was attributed to the lithium salt content of the studied electrolytes being optimized for PEO(LiTFSI) systems.<sup>45</sup>  $^1\text{H}$  diffusion coefficient was also measured using pulsed field gradient NMR with higher diffusion coefficients being indicative of greater polymer chain mobility.<sup>46</sup> Trends in proton diffusion coefficients were less

clear with diffusion in the PEO(LiTFSI)-LAGP samples being the same within error regardless of preparation method (Fig. 4). Proton diffusion coefficient was lowest in the MP PEO(LiBOB)-LAGP sample (Fig. 4). The highest diffusion coefficient was observed in the SC sample. These results show that local-scale proton diffusion due to polymer chain mobility is not significantly impacted by the presence of trace amounts of absorbed acetonitrile or even 30 000 to 40 000 ppm absorbed water. It also implies that ceramic particle agglomeration does not affect local-scale polymer chain mobility even if it has been shown to impact long-range ionic conductivity (Fig. 1).

As large differences in  $^1\text{H}$  mobility were not observed by NMR spectroscopy, it was concluded that local-scale polymer mobility may not be predictive of lithium ion conductivity which relies on a combination of polymer chain mobility and ion hopping.<sup>47</sup> Fig. 5 shows that the lowest ionic conductivities are observed in the WET hybrid electrolytes. The highest overall ionic conductivities are observed in the MP and ACE

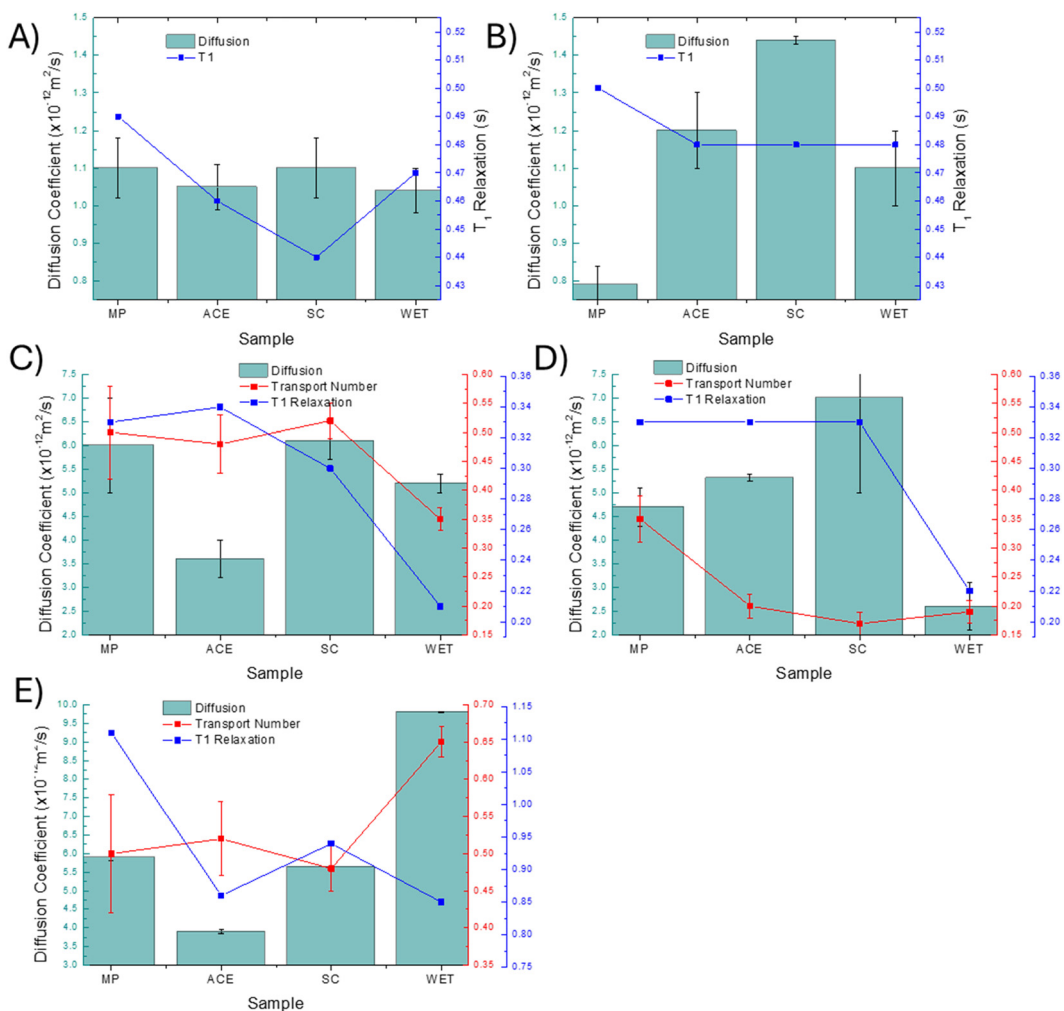


Fig. 4 Ion mobility at 60 °C as determined by solid-state NMR spectroscopy. (A) and (B) Represent proton mobility in PEO(LiTFSI)-LAGP and PEO(LiBOB)-LAGP samples respectively while (C) and (D) represent lithium mobility in PEO(LiTFSI)-LAGP and PEO(LiBOB)-LAGP respectively. (E) Represents fluorine mobility in PEO(LiTFSI)-LAGP. All spectra were acquired at 9.4 T with 5 kHz MAS. Lithium transport numbers for the LiBOB-containing samples were determined electrochemically using the Bruce–Vincent method.



electrolytes despite these having lower polymer chain mobility (Fig. 4). Ionic conductivities, which are the average of three measurements, in the MP and ACE samples are the same within error at all temperatures aside from 60 °C. This was attributed to LAGP dispersion having a more significant impact on ionic conductivity than trace amounts of acetonitrile. The difference in ionic conductivity between the MP and ACE samples was thought to be the result of the MP samples having a lower melting point (Fig. 3). Studies performed by Mangani *et al.* showed that pretreatment of a LATP surface with acetonitrile resulted in lower resistance across the polymer–ceramic interface when compared with a pristine LATP sample.<sup>36</sup> The ACE samples were not found to be more conductive than the MP samples (Fig. 5). This is either the result of acetonitrile not being detected on the treated ceramic by infrared spectroscopy (Fig. S6) or due to ionic conductivity occurring through the polymer phase only in the hybrid electrolytes presented in this work. Ionic conductivities in the LiBOB-containing MP, ACE and SC samples were lower than those in the LiTFSI-containing analogues below 60 °C. This was attributed to a previously observed interaction between LAGP and carbonates (like the BOB anion) where the formation of ion complexes can decrease salt mobility and therefore ionic conductivity.<sup>48</sup>

The observation of the highest ionic conductivity in the MP and ACE samples correlates with the data presented in Fig. 1 which shows that the solvent-free samples prepared by Cheng *et al.* and Piana *et al.* tended to be at least as conductive as the PEO–LAGP samples with the same LAGP content that were prepared *via* solution casting.<sup>8,9</sup> Water content measurements revealed that the WET samples contained far more water than the solution-casted, acetonitrile-soaked LAGP and melt-processed samples. They were also the only samples to contain significant quantities of acetonitrile (Fig. S5). The presence of absorbed solvents did not enhance ionic conductivity as the WET samples were the least conductive. These results show

that ceramic particle distribution likely has a greater impact on long-range ionic conductivity than polymer chain mobility and solvent absorption.

Differences in LAGP distribution between the MP, ACE SC and WET samples observed *via* SEM imaging (Fig. 2 and Fig. S1) indicate that tortuosity can be expected to be higher in the SC and WET samples. Ionic conductivities of the hybrid electrolytes were therefore compared to the ionic conductivities of the corresponding polymer electrolytes to determine the impact of LAGP distribution on ionic conductivity. Sample tortuosity, which is provided in Tables S1–S4, was calculated according to eqn (1) by comparing the ionic conductivity of PEO–LiTFSI and PEO–LiBOB (prepared *via* MP, ACE, SC and WET methods) ( $\sigma_{\text{optimal}}$ ) with the ionic conductivities of the respective hybrid electrolytes (Tables S1–S4) ( $\sigma_{\text{effective}}$ ).  $\varepsilon$  is the volume of PEO which was deemed to be the phase responsible for ionic conductivity in the hybrid electrolytes. PEO occupies 75% of the electrolyte volume.

$$\tau = \frac{\sigma_{\text{optimal}}}{\sigma_{\text{effective}}} \times \varepsilon \quad (1)$$

PEO was determined to be the conductive phase in the hybrid electrolytes *via* both impedance spectroscopy and NMR spectroscopy. The break in slope observed between 50 and 60 °C in Fig. 5 can be correlated with the  $T_m$  of PEO.<sup>24</sup> LAGP is not expected to undergo any phase transitions in the studied temperature range.<sup>49</sup> A linear ionic conductivity as a function of temperature plot would be expected if long-range ionic conductivity were to occur through the ceramic phase. An analysis of <sup>7</sup>Li diffusion in PEO–LAGP samples showed that lithium diffusion was about two orders of magnitude higher in the PEO phase than in the LAGP phase ( $10^{-12}$  vs.  $10^{-14} \text{ m}^2 \text{ s}^{-1}$ ). A more precise determination of the lithium ion diffusion coefficient in the LAGP phase was not possible as it was too low to quantify using pulsed field gradient NMR. Phase specific diffusion coefficients cannot be determined using electrochemical methods. In addition, the coating of ceramic particles by PEO during synthesis, during either melt processing or solution casting methods, is expected to make long-range direct contact between LAGP particles unlikely.

The ionic conductivity in a hybrid system could occur *via* an Arrhenius and/or a VTF (Vogel–Tamman–Fulcher) mechanism. Ion conduction is known to occur *via* the Arrhenius mechanism in ceramic electrolytes while the VTF mechanism, which accounts for the effect of polymer chain segmental motion, is typically used in pure PEO–LiTFSI. Devaux *et al.* showed that ionic conductivities in various PEO–LiTFSI electrolytes were best predicted using a VTF mechanism where molecular weight and end group type were also significant when the average molecular weight of the PEO was below about 10 000 M.<sup>50</sup> As the provided conductivity as a function of temperature plot does not show linear behaviour over the studied temperature range (Fig. 5), it can be concluded that the hybrid electrolytes presented here do not exhibit purely Arrhenius behaviour. Caradant *et al.* presented an analysis of the ion conduction mechanism in polymer blend electrolytes using Arrhenius, VTF

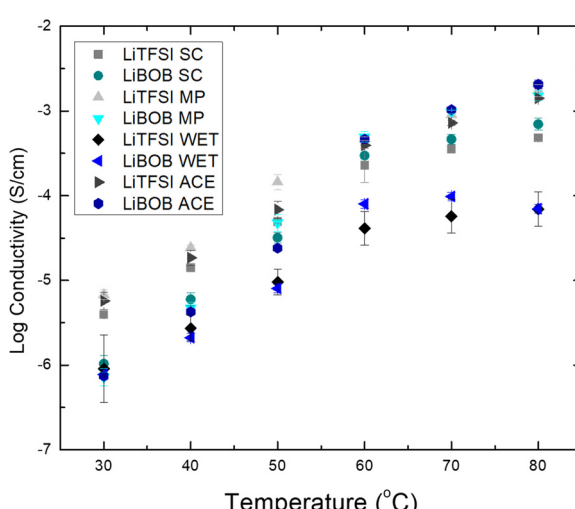


Fig. 5 Ionic conductivity of PEO(LiTFSI)–LAGP and PEO(LiBOB)–LAGP prepared *via* MP, ACE, SC and WET techniques. Ionic conductivities were measured between 30 and 80 °C.



and modified VTF models.<sup>51</sup> They showed that none of these models could be conclusively assigned to the polymer blend electrolytes. The PEO-LAGP hybrid electrolytes are predicted to be similar to the polymer blend electrolytes in the sense that the ionic conductivity occurs through a single phase, which in this case is PEO, whose crystallinity is influenced by the presence of LAGP particles and possibly the presence of acetonitrile depending on preparation method (Fig. 3). This is likely because, as stated by Devaux *et al.*, ion transfer by hopping in addition to polymer chain motion can occur in high molecular weight PEO.<sup>50</sup> The PEO used here and in the work by Caradant *et al.* has a molecular weight of 5 000 000 M. The ionic conductivity of the PEO-LAGP hybrid electrolytes would need to be investigated in greater detail in order to determine a precise mechanism for ionic conductivity and the possible impact of preparation method in these systems.

An analysis of the MP and ACE samples shows that LAGP addition generally improved ionic conductivity relative to a PEO polymer electrolyte, resulting in a tortuosity of less than 1 (Table S1). These results are demonstrative of the solid particles disrupting PEO crystallinity and thereby increasing the ionic conductivity of the hybrid electrolyte with respect to the PEO-LiTFSI and PEO-LiBOB polymer electrolytes (Table S1).<sup>52</sup> Well dispersed LAGP particles do not significantly increase tortuosity in the electrolyte. They were also correlated with a decrease in  $T_m$  (Fig. 3). Greater increases in tortuosity were observed for the SC samples, particularly under 60 °C, where tortuosity ranging from about 10–20 was observed (Table S2). Lower tortuosity at higher temperatures was attributed to lower PEO crystallinity. The highest tortuosity was observed in the WET samples (Table S3). With the exception of the drying procedure, the same preparation steps were used to make the WET and SC samples. LAGP dispersion in the WET and SC hybrid electrolytes should therefore be about the same. Yet, Fig. 5 and Tables S2, S3 show that ionic conductivity is lower in both the WET hybrid electrolytes and the WET solid polymer electrolytes. The most significant difference between the WET and SC samples is that the WET samples contain NMR-detectable quantities of acetonitrile whereas the SC samples do not. Hakem *et al.* have shown that acetonitrile can reduce lithium ion mobility by causing the ions to bind to the PEO polymer chains, thereby reducing long-range ionic conductivity.<sup>14</sup> Müller *et al.* have additionally shown that residual acetonitrile can cause PEO decomposition in the presence of lithium metal.<sup>53</sup> Although lithium metal was not present in the cells that were used to measure ionic conductivity, some interaction between PEO and acetonitrile due to the application of heat and electrical current may be possible. These results correlate with the data presented in Fig. 1 which show that preparation methods that decrease ceramic particle agglomeration result in higher ionic conductivity. Additionally, the presence of excessive water and acetonitrile does not improve ionic conductivity in the hybrid electrolytes as it appears to be negated by poor LAGP distribution due to solution casting. Tortuosity was slightly higher in the ACE samples than in the MP samples. Although no acetonitrile was detected in the ACE samples (Fig. S6). The full impact of acetonitrile on the ionic

conductivity of the samples presented in Fig. 1 cannot be evaluated as none of the authors provided any information regarding the quantity of this solvent in their electrolyte samples.

<sup>7</sup>Li NMR was performed to compare lithium ion mobility in the hybrid electrolytes that were prepared *via* melt-processing and solution-casting. The hybrid electrolytes contain two lithium environments corresponding to lithium salt in the PEO matrix and lithium in LAGP. These peaks overlap significantly with the lithium salt in PEO peak being located at –0.47 ppm and the LAGP peak being located at –0.52 ppm (Fig. S7). Both peaks can be extracted from the one-dimensional <sup>7</sup>Li spectrum of the hybrid electrolyte *via* peak fitting but are observed with better resolution following pulsed field gradient NMR (Fig. S7). The improvement in resolution allowed local-scale lithium ion mobility in both phases to be compared. Analysis of the pulsed field gradient spectra showed that the lithium ions in the polymer phase were more mobile as their diffusion coefficients were about two orders of magnitude higher. Lithium diffusion coefficients of the LAGP phase were on the order of  $10^{-14} \text{ m}^2 \text{ s}^{-1}$ , making them difficult to accurately quantify with the available NMR equipment. It is for this reason that the lithium diffusion coefficients and transport numbers that are reported in Fig. 4 correspond to the PEO phase only. In addition, the low lithium ion mobility in the ceramic phase observed by <sup>7</sup>Li NMR supports the conclusions that were made based on the analysis of Fig. 5: long range ionic conductivity occurs through the polymer phase only.

Fig. 4 shows that <sup>7</sup>Li  $T_1$  relaxation times at 60 °C are similar in the MP, ACE and SC samples but are reduced by about 0.1 s in the WET samples.  $T_1$  relaxation time can be linked to motional processes with lower relaxation times generally being indicative of higher ion mobility.<sup>54,55</sup> The faster  $T_1$  relaxation observed in the WET samples provides some contrast with the ionic conductivity data (Fig. 5) which shows that the WET hybrid electrolytes are the least conductive. This observation can be reconciled by considering that ionic conductivity is a long-range process (motion of lithium ions across an electrolyte) whereas NMR measures local-scale processes. This indicates higher local-scale lithium ion mobility in the WET samples despite lower ionic conductivity in the bulk electrolyte. This likely results from the impact of absorbed water increasing lithium ion mobility in these samples while the more long-range effects of LAGP particle agglomeration hindering lithium ion mobility are not observed at the NMR measurement scale.

Lithium ion diffusion coefficients were determined *via* pulsed field gradient NMR to provide an additional measure of lithium ion mobility in the hybrid electrolytes (Fig. 4). The provided lithium diffusion coefficients correspond to the PEO phase only as the lithium diffusion coefficients in the LAGP phase were too low to properly quantify. Lithium diffusion coefficients were about the same within error for the LiTFSI-containing samples with the SC sample having the highest average value (Fig. 4). Similar results were observed for the LiBOB-containing samples where the SC sample had the highest average diffusion coefficient and was the same as the MP sample within error (Fig. 4). The WET samples had the lowest average diffusion coefficients for the PEO(LiBOB) samples



which correlates with the observed ionic conductivities (Fig. 5). The ACE sample had the lowest lithium diffusion coefficient for the PEO(LiTFSI) samples despite its higher ionic conductivity. Increases in ionic conductivity relative to the SC and WET samples were likely related to decreased tortuosity improving long-range lithium ion mobility.

Lithium transport numbers in the LiTFSI-containing electrolytes were calculated from the  $^{7}\text{Li}$  and  $^{19}\text{F}$  diffusion coefficients determined *via* pulsed field gradient NMR (Fig. 4). The  $^{7}\text{Li}$  transport number of the LAGP phase was not provided as LAGP is a single ion conductor with a theoretical lithium ion transport number of 1.<sup>9</sup> The lithium transport numbers for the PEO(LiTFSI) samples were 0.50, 0.48 and 0.52 for the melt-processed, ACE and solution-casted samples respectively which was significantly higher than the 0.35 that was observed for the WET sample (Fig. 4). The lithium transport number in the PEO-LiTFSI solid polymer electrolyte was determined to be  $0.21 \pm 0.02$  *via* PFG NMR. The presence of ceramic particles therefore improves local-scale lithium ion mobility even though particle agglomeration in solution-casted samples results in decreased ionic conductivity relative to the corresponding solid polymer electrolyte. The effects of particle agglomeration were therefore determined to primarily affect long-range processes like ion conductivity whereas local-scale ion mobility was mostly influenced by changes in polymer chain mobility.

Lithium transport numbers in PEO(LiBOB)-LAGP were determined electrochemically using the Bruce–Vincent method. This was done because a transport number for the BOB anion could not be easily measured *via* NMR. The spin-lattice and spin–spin relaxations of  $^{10}\text{B}$  and  $^{11}\text{B}$  were too fast to allow for adequate delay time between gradient pulses and the abundancies of  $^{13}\text{C}$  and  $^{17}\text{O}$  were too low to obtain adequate signal following the application of a gradient pulse. The main difference between the Bruce–Vincent method (bulk lithium ion transport) and PFG NMR (local-scale ion transport) must be taken into account when analyzing this data. The lithium ion transport number in MP PEO(LiBOB)-LAGP, 0.35, was significantly higher than those of the SC, ACE and WET samples which were 0.17, 0.20 and 0.19 respectively (Fig. 4). This was linked to improved lithium ion mobility due to the absence of LAGP particle agglomeration in the MP sample compared to the SC and WET samples. The observed increase in lithium ion mobility relative to the ACE sample may be the result of the incorporation of small amounts of acetonitrile in the PEO phase reacting with the lithium metal electrodes despite not being able to detect the solvent *via* IR, NMR or DSC methods. The difference in measuring technique means that the lithium ion diffusion coefficients in the LiTFSI and the LiBOB samples cannot be directly compared.

The impact of sample preparation method on stability with respect to lithium metal electrodes was evaluated by performing cycling in Li–Li cells. Electrolytes were cycled in symmetric Li–PEO–hybrid–PEO–Li cells for 325 h at 60 °C with a current density of 0.05 mA cm<sup>−2</sup>. Current was applied in 30-minute increments. PEO electrolyte layers (made with either LiTFSI or LiBOB) were placed between the hybrid electrolyte and the lithium electrodes to prevent reactivity between LAGP and the

lithium electrode.<sup>25</sup> These protective layers were also prepared using the MP, SC, ACE and WET methods. The stability of the system was evaluated by acquiring impedance spectra every 50 cycles. These spectra show that LiBOB-containing samples tended to be more stable over time than the LiTFSI-containing samples (Fig. 6 and 7).

Fig. S8 shows Li–Li cycling curves for PEO(LiBOB)-LAGP samples. The MP, ACE and SC samples show similar stability. This is linked to these samples being similar: low water content and no detectable acetonitrile in the SC sample. The WET PEO(LiBOB)-LAGP sample has similar stability but a potential difference of 0.35–0.4 V as opposed to ~0.04 V is observed (Fig. S8). The higher voltage, coupled with greater resistance in the impedance plots (Fig. 6) suggests lower stability at the electrolyte–lithium metal interface. Long-term stability in a symmetric Li–Li cell was also evaluated in PEO(LiTFSI)-LAGP (Fig. 7). Samples prepared with LiTFSI were found to be less stable over time and have higher interfacial resistance than those that were prepared with LiBOB regardless of preparation method (Fig. S9 and Fig. 6). The BOB anion has previously been shown to have a stabilizing effect as it can form complexes with PEO-type electrolytes that have a higher electrochemical stability than PEO alone.<sup>19,56</sup> This was verified by the authors by testing the electrochemical stability of PEO(LiBOB) and PEO(LiTFSI) with respect to lithium metal *via* potentiostatic intermittent titration technique. PEO(LiTFSI) electrolytes were found to be stable up to 3.75 V whereas PEO(LiBOB) electrolytes were found to be stable up to 3.9 V. As LAGP has independently been found to be stable up to 4.9 V *via* the potentiostatic intermittent titration technique,<sup>57</sup> it is anticipated that the electrochemical stability of this system is limited by the stability of the polymer phase.

More significant differences in the resistance of the lithium metal–polymer electrolyte interface were observed between the preparation methods for the LiTFSI-containing hybrid electrolytes than for the LiBOB-containing electrolytes. The MP PEO(LiTFSI)-LAGP sample was more stable than those that were prepared *via* the other methods (Fig. 7 and Fig. S9). Relatively small increases in resistance and voltage were observed between the MP, ACE and SC samples whereas large lithium–electrolyte interfacial resistances and voltages above 3 V were observed for the WET samples (Fig. 7 and Fig. S9). The high interfacial resistance in the WET sample was attributed to a reaction between residual acetonitrile and deposited lithium that results in the formation of alkyl-lithium species.<sup>53</sup> The alkyl-lithium species can then react further with residual water inside the PEO electrolyte to produce LiOH which can then cleave ether bonds within the polymer.<sup>53</sup> This phenomenon is most likely to occur in the WET samples as they contain the greatest amount of water and acetonitrile. The MP samples contain no acetonitrile and are thus the most stable during cycling in Li–Li cells. These results contrast with those presented in Table 2 which show that solution-casted samples were cycled at the highest current densities. It is however difficult to compare samples that were analyzed under different conditions, where the presence of residual water or casting



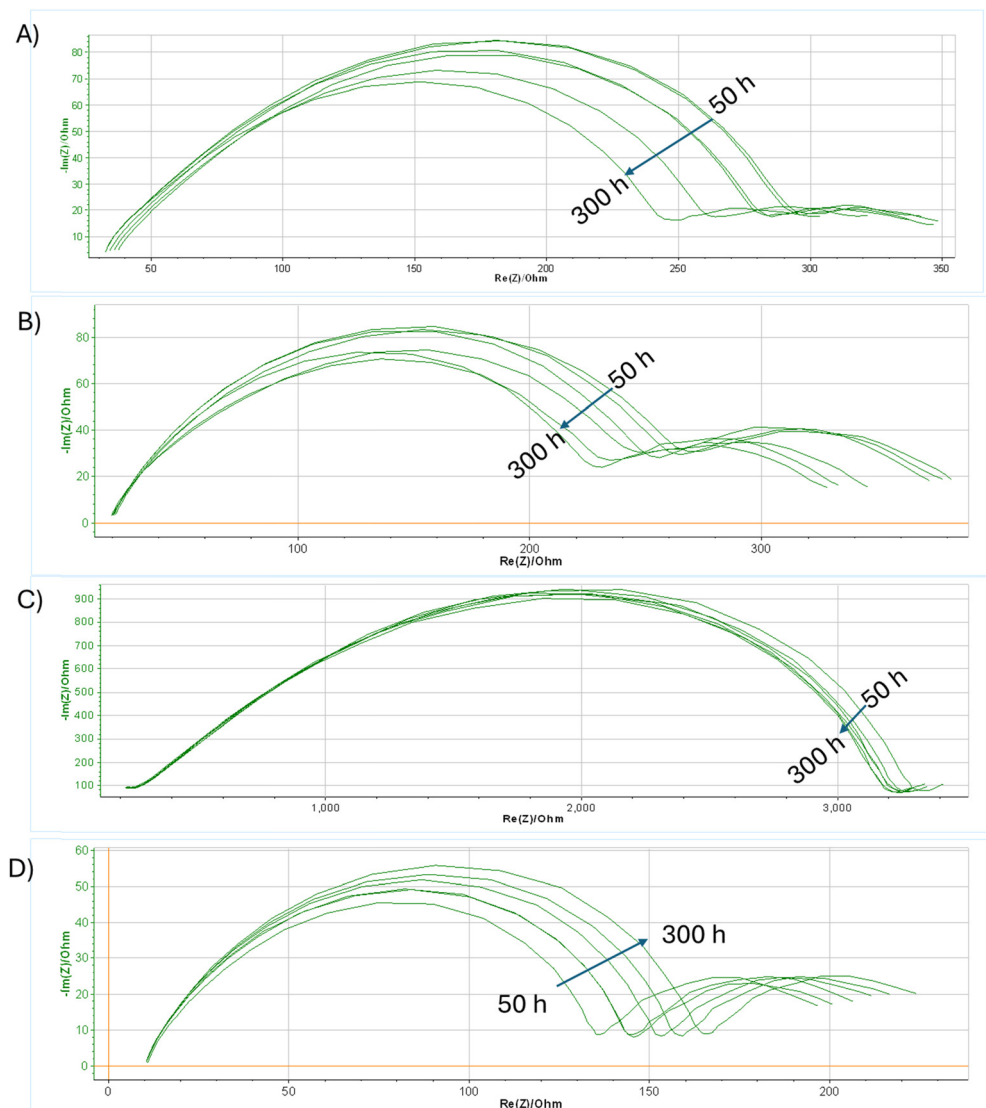


**Fig. 6** Impedance spectra of PEO(LiBOB)-LAGP following cycling in Li–Li symmetric cells at 60 °C for a period spanning 50 to 300 hours. The spectra presented in (A) correspond to the MP sample, the spectra presented in (B) correspond to the SC sample, the spectra presented in (C) correspond to the WET sample and the spectra presented in (D) correspond to the ACE sample.

solvent was not declared or quantified, making this study a more reliable evaluation of the effects of solution casting on electrolyte performance. Stabilization of the polymer–lithium interface *via* the decomposition of LiBOB is expected to be responsible for the greater stability observed in the LiBOB-containing samples.

This study shows that in PEO–LAGP hybrid electrolytes that contain 50 wt% PEO/LAGP, electrolyte properties including morphology, polymer mobility, ion conductivity and stability with respect to lithium metal depend on preparation method. Even though a specific system was investigated, two major conclusions were found that can be applied to hybrid electrolytes more broadly. Solution casting, which was associated with LAGP particle agglomeration in the hybrid electrolytes, resulted in poorer ceramic particle distribution. These differences in morphology increased sample tortuosity which resulted in lower

ionic conductivity when compared to the samples that were prepared *via* the MP and ACE methods where melt extrusion was used. The impact of solution casting on ceramic particle dispersion in polymer–ceramic hybrid electrolytes is expected to be relevant for other systems, irrespective of the polymer and ceramic powder in question. The impact is expected to be greater in samples containing higher proportions of ceramic, as demonstrated in Fig. 1 where electrolytes containing high proportions of ceramic tended to have lower ionic conductivities. Significant ceramic particle agglomeration was found to have a more significant impact on ionic conductivity than plasticization by absorbed water and/or acetonitrile as higher local-scale polymer and lithium ion mobility, as observed by NMR spectroscopy, did not translate to increased ionic conductivity.

The presence of acetonitrile and water in the WET samples had a significant impact on the stability of these samples.

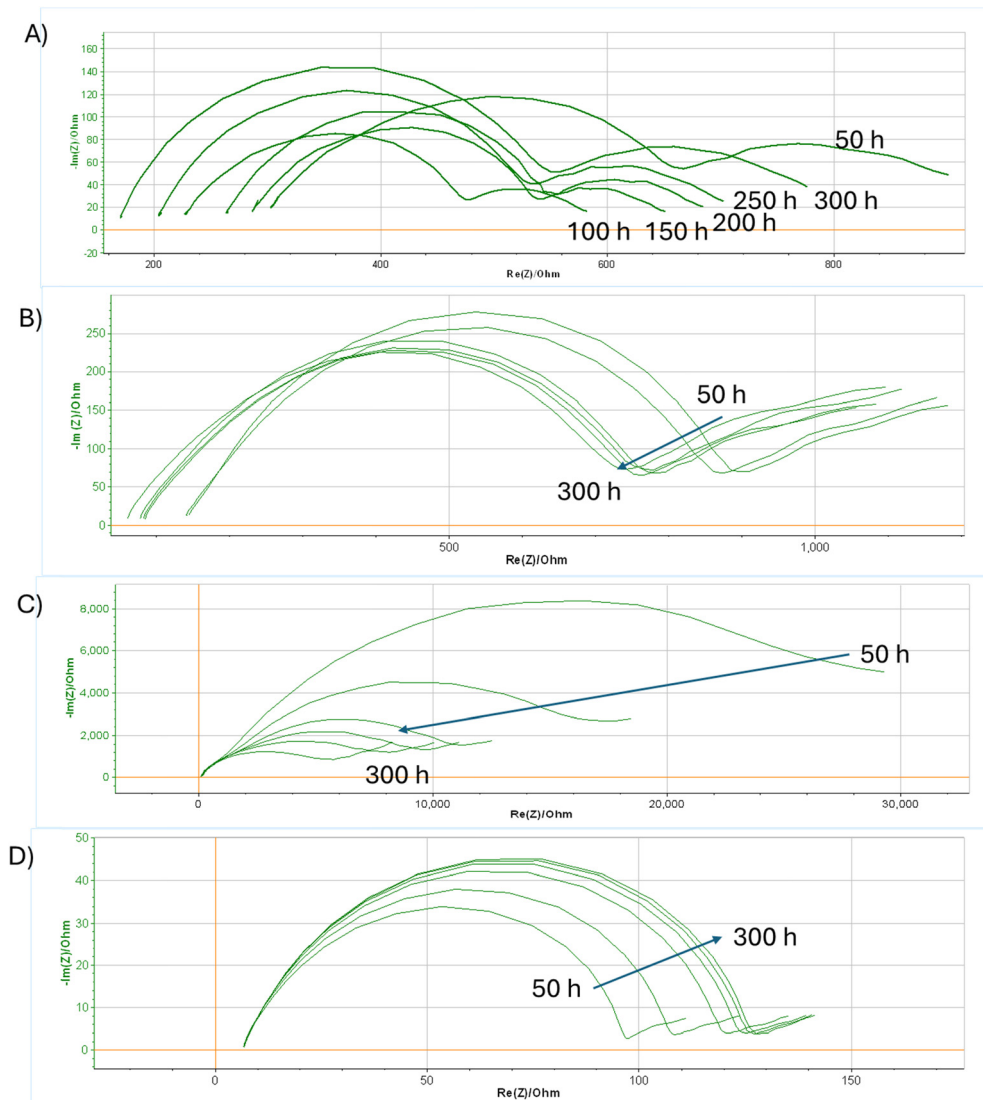


**Fig. 7** Impedance spectra of PEO(LiTFSI)-LAGP following cycling in Li-Li symmetric cells at 60 °C for a period spanning 50 to 300 hours. The spectra presented in (A) correspond to the MP sample, the spectra presented in (B) correspond to the SC sample, the spectra presented in (C) correspond to the WET sample and the spectra presented in (D) correspond to the ACE sample.

These solvents were associated with the partial decomposition of LiBOB salt which was observed *via* DSC, NMR and infrared spectroscopies. The WET samples were also observed to be less stable with respect to lithium metal during cycling in Li-Li cells. This contrasts with the data presented in Table 2 wherein hybrid electrolytes prepared *via* solution casting are not shown to be less stable during cycling in Li-Li cells than those that were prepared *via* hot pressing. It is however not possible to evaluate the cited systems in terms of solvent content as this information was not provided by the authors. These results can be extrapolated to suggest that the presence of significant quantities of residual solvent negatively impacts the stability of both hybrid and polymer electrolytes, especially when these are integrated into battery systems, as observed by Huttner *et al.* through the evaluation of water content in electrodes and separators in lithium ion batteries.<sup>58</sup> Although the type and quantities of polymer and ceramic are expected to influence

solvent uptake and ease of drying in hybrid electrolytes, these findings highlight the impact of preparation method in minimizing solvent content in all hybrid electrolytes.

## Conclusion

Previously published examples of PEO-LAGP hybrid electrolytes prepared by solution casting and solvent-free processing methods were compared. Although comparing the performance of electrolytes that were made under different conditions was difficult, several conclusions could be made. A general trend of higher ionic conductivity at lower ceramic loadings was observed. This was linked to lower tortuosity allowing for better ionic conductivity through the conductive polymeric phase. SEM images provided by some of the cited authors showed that solvent-free preparation methods resulted in better ceramic particle distribution. Overall, the differences between



samples made it difficult to definitively compare the impact of solution casting and solvent-free polymer electrolyte preparation techniques on electrolyte performance. PEO-LAGP samples were therefore prepared *via* solution casting and solvent-free melt processing methods. These samples were made from the same starting materials and contained the same proportions of polymer and ceramic. The solution-casted samples were further subdivided into two categories. SC samples that were dried under vacuum prior to use and WET samples that only underwent evaporation in a fume hood. As observed in the literature, MP preparation resulted in better LAGP dispersion in the hybrid electrolytes which resulted in lower tortuosity and higher ionic conductivity than in the SC and WET samples. Local-scale lithium ion mobility was less impacted by preparation method than long-range transport which was hindered by LAGP particle agglomeration in the SC and WET samples. The MP hybrids were more conductive than the corresponding solid polymer electrolytes. The preparation of ACE hybrid electrolytes, prepared by melt processing using LAGP that was pre-exposed to acetonitrile, showed that LAGP particle dispersion had a greater influence on electrochemical performance than the presence of small amounts of absorbed solvent. Very similar behaviour with regards to lithium mobility was observed by impedance and NMR spectroscopies for these samples. An increase in ionic conductivity was not observed for the hybrid samples prepared using SC methods which suggests that this observation may be linked to significant particle agglomeration negating the reduction in polymer chain crystallization and boost in ionic conductivity that are often reported for hybrid electrolyte systems. Ionic conductivity was concluded to occur through the polymer phase only in all cases. Residual acetonitrile, which was observed in the WET samples only, was linked to lower interfacial stability with lithium metal. As absorbed acetonitrile does not have a substantial plasticising effect in PEO, the WET samples were not more conductive than the MP and SC samples. In addition to deteriorating sample morphology, electrolyte preparation *via* solution casting is more time consuming and is expected to be more expensive on a large scale because of the significant quantities of solvent that are needed in addition to the costs that are associated with evaporation and recycling. It is therefore recommended that ceramic-in-polymer hybrid electrolytes be prepared *via* solvent-free methods as the samples have been shown to be more conductive and more stable with respect to lithium metal during long-term cycling. In addition, the use of LiBOB was found to result in improved stability at the electrolyte–lithium metal interface during cycling with lithium when compared to electrolytes that were prepared with the more commonly used LiTFSI.

## Author contributions

Gabrielle Foran: writing original draft, writing review and editing, investigation, methodology, conceptualization, data curation. Cédric Barcha: writing review and editing, conceptualization.

Caroline St-Antoine: investigation, methodology. Arnaud Prébé: funding acquisition, writing review and editing, project administration, supervision, Mickael Dollé: funding acquisition, writing review and editing, project administration, supervision, resources.

## Conflicts of interest

There are no conflicts of interest to declare.

## Data availability

The data supporting this article have been included as part of the SI.

SEM images, DSC, IR and NMR spectra, cycling curves for Li–Li cells and tortuosity calculations. See DOI: <https://doi.org/10.1039/d5ya00082c>

## Acknowledgements

The authors would like to acknowledge funding from the Natural Science and Engineering Research Council of Canada (NSERC) and TotalEnergies Canada Inc. (NSERC Collaborative Research and Development RDCPJ 528052-18) and support from FRQ-Secteur NT – Strategic Clusters (RS-265155). The authors would also like to acknowledge the staff of the NMR facility, the Maples characterization platform and the Laboratoire de caractérisation des matériaux at the Université de Montréal for assistance with sample characterization.

## References

- 1 C. Yan, P. Zhu, H. Jia, Z. Du, J. Zhu, R. Orenstein, H. Cheng, N. Wu, M. Dirican and X. Zhang, Garnet-Rich Composite Solid Electrolytes for Dendrite-Free, High-Rate, Solid-State Lithium-Metal Batteries, *Energy Storage Mater.*, 2020, **26**, 448–456, DOI: [10.1016/j.ensm.2019.11.018](https://doi.org/10.1016/j.ensm.2019.11.018).
- 2 L. Chen, Y. Li, S.-P. Li, L.-Z. Fan, C.-W. Nan and J. B. Goodenough, PEO/Garnet Composite Electrolytes for Solid-State Lithium Batteries: From “Ceramic-in-Polymer” to “Polymer-in-Ceramic”, *Nano Energy*, 2018, **46**, 176–184, DOI: [10.1016/j.nanoen.2017.12.037](https://doi.org/10.1016/j.nanoen.2017.12.037).
- 3 W. Liu, S. W. Lee, D. Lin, F. Shi, S. Wang, A. D. Sendek and Y. Cui, Enhancing Ionic Conductivity in Composite Polymer Electrolytes with Well-Aligned Ceramic Nanowires, *Nat. Energy*, 2017, **2**(5), 17035, DOI: [10.1038/nenergy.2017.35](https://doi.org/10.1038/nenergy.2017.35).
- 4 J. A. Isaac, D. Devaux and R. Bouchet, Dense Inorganic Electrolyte Particles as a Lever to Promote Composite Electrolyte Conductivity, *Nat. Mater.*, 2022, **21**, 1412–1418, DOI: [10.1038/s41563-022-01343-w](https://doi.org/10.1038/s41563-022-01343-w).
- 5 A. Méry, S. Rousselot, D. Lepage, D. Aymé-Perrot and M. Dollé, Limiting Factors Affecting the Ionic Conductivities of LATP/Polymer Hybrid Electrolytes, *Batteries*, 2023, **9**(2), 87, DOI: [10.3390/batteries9020087](https://doi.org/10.3390/batteries9020087).
- 6 M. Liu, Z. Cheng, S. Ganapathy, C. Wang, L. A. Haverkate, M. Tułodziecki, S. Unnikrishnan and M. Wagemaker,

Tandem Interface and Bulk Li-Ion Transport in a Hybrid Solid Electrolyte with Microsized Active Filler, *ACS Energy Lett.*, 2019, **4**(9), 2336–2342, DOI: [10.1021/acsenergylett.9b01371](https://doi.org/10.1021/acsenergylett.9b01371).

7 J. Zagórska, J. M. López Del Amo, M. J. Cordill, F. Aguesse, L. Buannic and A. Llordés, Garnet-Polymer Composite Electrolytes: New Insights on Local Li-Ion Dynamics and Electrodeposition Stability with Li Metal Anodes, *ACS Appl. Energy Mater.*, 2019, **2**(3), 1734–1746, DOI: [10.1021/acsaelm.8b01850](https://doi.org/10.1021/acsaelm.8b01850).

8 J. Cheng, G. Hou, Q. Sun, Z. Liang, X. Xu, J. Guo, L. Dai, D. Li, X. Nie, Z. Zeng, P. Si and L. Ci, Cold-Pressing PEO/LAGP Composite Electrolyte for Integrated All-Solid-State Lithium Metal Battery, *Solid State Ionics*, 2020, **345**, 115156, DOI: [10.1016/j.ssi.2019.115156](https://doi.org/10.1016/j.ssi.2019.115156).

9 G. Piana, F. Bella, F. Geobaldo, G. Meligrana and C. Gerbaldi, PEO/LAGP Hybrid Solid Polymer Electrolytes for Ambient Temperature Lithium Batteries by Solvent-Free, “One Pot” Preparation, *J. Energy Storage*, 2019, **26**, 100947, DOI: [10.1016/j.est.2019.100947](https://doi.org/10.1016/j.est.2019.100947).

10 K. Pożyczka, M. Marzantowicz, J. R. Dygas and F. Krok, Ionic Conductivity and Lithium Transfer Number Of Poly(Ethylene Oxide):LITFSI System, *Electrochim. Acta*, 2017, **227**, 127–135, DOI: [10.1016/j.electacta.2016.12.172](https://doi.org/10.1016/j.electacta.2016.12.172).

11 J. Zheng, M. Tang and Y.-Y. Y. Hu, Lithium Ion Pathway within  $\text{Li}_7\text{La}_3\text{Zr}_2\text{O}_{12}$ –Polyethylene Oxide Composite Electrolytes, *Angew. Chem., Int. Ed.*, 2016, **55**(40), 12538–12542, DOI: [10.1002/anie.201607539](https://doi.org/10.1002/anie.201607539).

12 J. E. Weston and B. C. H. Steele, Effects of Preparation Method on Properties of Lithium Salt–Poly(Ethylene Oxide) Polymer Electrolytes, *Solid State Ionics*, 1982, **7**(1), 81–88, DOI: [10.1016/0167-2738\(82\)90073-X](https://doi.org/10.1016/0167-2738(82)90073-X).

13 B. Commarieu, A. Paolella, S. Collin-Martin, C. Gagnon, A. Vlijh, A. Guerfi and K. Zaghib, Solid-to-Liquid Transition of Polycarbonate Solid Electrolytes in Li-Metal Batteries, *J. Power Sources*, 2019, **436**, 226852, DOI: [10.1016/j.jpowsour.2019.226852](https://doi.org/10.1016/j.jpowsour.2019.226852).

14 I. F. Hakem, J. Lal and M. R. Brockstaller, Mixed Solvent Effect on Lithium-Coordination to Poly(Ethylene Oxide), *J. Polym. Sci., Part B: Polym. Phys.*, 2006, **44**, 3642–3650, DOI: [10.1002/polb.21014](https://doi.org/10.1002/polb.21014).

15 A. K. Łasińska, M. Marzantowicz, J. R. Dygas, F. Krok, Z. Florjańczyk, A. Tomaszewska, E. Zygałdo-Monikowska, Z. Zukowska and U. Lafont, Study of Ageing Effects in Polymer-in-Salt Electrolytes Based on Poly(Acrylonitrile-Co-Butyl Acrylate) and Lithium Salts, *Electrochim. Acta*, 2015, **169**, 61–72, DOI: [10.1016/j.electacta.2015.04.023](https://doi.org/10.1016/j.electacta.2015.04.023).

16 B. Sun, J. Mindemark, K. Edström and D. Brandell, Polycarbonate-Based Solid Polymer Electrolytes for Li-Ion Batteries, *Solid State Ionics*, 2014, **262**, 738–742, DOI: [10.1016/j.ssi.2013.08.014](https://doi.org/10.1016/j.ssi.2013.08.014).

17 D. Mankovsky, D. Lepage, M. Lachal, L. Caradant, D. Aymé-Perrot and M. Dollé, Water Content in Solid Polymer Electrolytes: The Lost Knowledge, *Chem. Commun.*, 2020, **56**(70), 10167–10170, DOI: [10.1039/D0CC03556D](https://doi.org/10.1039/D0CC03556D).

18 S. Choudhury, Z. Tu, A. Nijamudheen, M. J. Zachman, S. Stalin, Y. Deng, Q. Zhao, D. Vu, L. F. Kourkoutis, J. L. Mendoza-Cortes and L. A. Archer, Stabilizing Polymer Electrolytes in High-Voltage Lithium Batteries, *Nat. Commun.*, 2019, **10**(1), 1–11, DOI: [10.1038/s41467-019-11015-0](https://doi.org/10.1038/s41467-019-11015-0).

19 Y. Wang, L. Xing, X. Tang, X. Li, W. Li, B. Li, W. Huang, H. Zhou and X. Li, Oxidative Stability and Reaction Mechanism of Lithium Bis(Oxalate)Borate as a Cathode Film-Forming Additive for Lithium Ion Batteries, *RSC Adv.*, 2014, **4**(63), 33301–33306, DOI: [10.1039/c4ra03018d](https://doi.org/10.1039/c4ra03018d).

20 K. Xu, S. Zhang, T. R. Jow, W. Xu and C. A. Angell, LiBOB as Salt for Lithium-Ion Batteries. A Possible Solution for High Temperature Operation, *Electrochem. Solid-State Lett.*, 2002, **5**(1), 1–5, DOI: [10.1149/1.1426042](https://doi.org/10.1149/1.1426042).

21 E. Zhao, F. Ma, Y. Guo and Y. Jin, Stable LATP/LAGP Double-Layer Solid Electrolyte Prepared: Via a Simple Dry-Pressing Method for Solid State Lithium Ion Batteries, *RSC Adv.*, 2016, **6**(95), 92579–92585, DOI: [10.1039/c6ra19415j](https://doi.org/10.1039/c6ra19415j).

22 J. Lee, T. Howell, M. Rottmayer, J. Boeckl and H. Huang, Free-Standing PEO/LiTFSI/LAGP Composite Electrolyte Membranes for Applications to Flexible Solid-State Lithium-Based Batteries, *J. Electrochem. Soc.*, 2019, **166**(2), A416–A422, DOI: [10.1149/2.1321902jes](https://doi.org/10.1149/2.1321902jes).

23 J. Lee, M. Rottmayer and H. Huang, Impacts of Lithium Salts on the Thermal and Mechanical Characteristics in the Lithiated PEO/LAGP Composite Electrolytes, *J. Compos. Sci.*, 2022, **6**(1), 1–9, DOI: [10.3390/jcs6010012](https://doi.org/10.3390/jcs6010012).

24 Y. Zhao, Z. Huang, S. Chen, B. Chen, J. Yang, Q. Zhang, F. Ding, Y. Chen and X. Xu, A Promising PEO/LAGP Hybrid Electrolyte Prepared by a Simple Method for All-Solid-State Lithium Batteries, *Solid State Ionics*, 2016, **295**, 65–71, DOI: [10.1016/j.ssi.2016.07.013](https://doi.org/10.1016/j.ssi.2016.07.013).

25 C. Wang, Y. Yang, X. Liu, H. Zhong, H. Xu, Z. Xu, H. Shao and F. Ding, Suppression of Lithium Dendrite Formation by Using LAGP–PEO (LiTFSI) Composite Solid Electrolyte and Lithium Metal Anode Modified by PEO (LiTFSI) in All-Solid-State Lithium Batteries, *ACS Appl. Mater. Interfaces*, 2017, **9**(15), 13694–13702, DOI: [10.1021/acsami.7b00336](https://doi.org/10.1021/acsami.7b00336).

26 J. Liu, W. Fang, S. Gao, Y. Chen, S. Chen, C. Hu, S. Cai, Z. Liu and X. Liu, Contactless Electric-Field Driven Z-Alignment of Ceramic Nanoparticles in Polymer Electrolyte to Enhance Ionic Conductivity, *Mater. Des.*, 2020, **192**, 108753, DOI: [10.1016/j.matdes.2020.108753](https://doi.org/10.1016/j.matdes.2020.108753).

27 X. Wang, H. Zhai, B. Qie, Q. Cheng, A. Li, J. Borovilas, B. Xu, C. Shi, T. Jin, X. Liao, Y. Li, X. He, S. Du, Y. Fu, M. Dontigny, K. Zaghib and Y. Yang, Rechargeable Solid-State Lithium Metal Batteries with Vertically Aligned Ceramic Nanoparticle/Polymer Composite Electrolyte, *Nano Energy*, 2019, **60**, 205–212, DOI: [10.1016/j.nanoen.2019.03.051](https://doi.org/10.1016/j.nanoen.2019.03.051).

28 J. Ou, G. Li and Z. Chen, Improved Composite Solid Electrolyte through Ionic Liquid-Assisted Polymer Phase for Solid-State Lithium Ion Batteries, *J. Electrochem. Soc.*, 2019, **166**(10), A1785–A1792, DOI: [10.1149/2.0401910jes](https://doi.org/10.1149/2.0401910jes).

29 Y. Liang, N. Chen, F. Li and R. Chen, Melamine-Regulated Ceramic/Polymer Electrolyte Interface Promotes High Stability in Lithium-Metal Battery, *ACS Appl. Mater. Interfaces*, 2022, **14**(42), 47822–47830, DOI: [10.1021/acsami.2c14940](https://doi.org/10.1021/acsami.2c14940).

30 J. Bu, P. Leung, C. Huang, S. H. Lee and P. S. Grant, Co-Spray Printing of  $\text{LiFePO}_4$  and PEO- $\text{Li}_{1.5}\text{Al}_{0.5}\text{Ge}_{1.5}(\text{PO}_4)_3$



Hybrid Electrodes for All-Solid-State Li-Ion Battery Applications, *J. Mater. Chem. A*, 2019, **7**(32), 19094–19103, DOI: [10.1039/c9ta03824h](https://doi.org/10.1039/c9ta03824h).

- 31 A. Caravella, S. Hara, A. Obuchi and J. Uchisawa, Role of the Bi-Dispersion of Particle Size on Tortuosity in Isotropic Structures of Spherical Particles by Three-Dimensional Computer Simulation, *Chem. Eng. Sci.*, 2012, **84**, 351–371, DOI: [10.1016/j.ces.2012.08.050](https://doi.org/10.1016/j.ces.2012.08.050).
- 32 S. Toe, J.-C. Remigy, L. Leveau, F. Chauvet, Y. Kerdja and T. Tzedakis, Investigating the Physical State of Polymer Electrolyte: Influence of Temperature and LiTFSI Concentration on the Phase of the Different States of the Polymer Electrolyte PEO-LiTFSI, *ECS Adv.*, 2023, **2**(4), 040509, DOI: [10.1149/2754-2734/ad119d](https://doi.org/10.1149/2754-2734/ad119d).
- 33 G. Foran, A. Mery, M. Bertrand, S. Rousselot, D. Lepage, D. Aymé-Perrot and M. Dollé, NMR Study of Lithium Transport in Liquid-Ceramic Hybrid Solid Composite Electrolytes, *ACS Appl. Mater. Interfaces*, 2022, **14**(38), 43226–43236, DOI: [10.1021/acsami.2c10666](https://doi.org/10.1021/acsami.2c10666).
- 34 G. Foran, D. Mankovsky, N. Verdier, D. Lepage, A. Prébé, D. Aymé-Perrot and M. Dollé, The Impact of Absorbed Solvent on the Performance of Solid Polymer Electrolytes for Use in Solid-State Lithium Batteries, *iScience*, 2020, **23**(10), 101597, DOI: [10.1016/j.isci.2020.101597](https://doi.org/10.1016/j.isci.2020.101597).
- 35 R. Sahore, Z. Du, X. C. Chen, W. B. Hawley, A. S. Westover and N. J. Dudney, Practical Considerations for Testing Polymer Electrolytes for High-Energy Solid-State Batteries, *ACS Energy Lett.*, 2021, **6**, 2240–2247, DOI: [10.1021/acsenergylett.1c00810](https://doi.org/10.1021/acsenergylett.1c00810).
- 36 L. R. Mangani, D. Devaux, A. Benayad, C. Jordy and R. Bouchet, Tuning Ceramic Surface to Minimize the Ionic Resistance at the Interface between PEO- and LATP-Based Ceramic Electrolyte, *ACS Appl. Mater. Interfaces*, 2024, **16**(34), 45713–45723, DOI: [10.1021/acsami.4c08882](https://doi.org/10.1021/acsami.4c08882).
- 37 P. Szymoniak, Z. Li, D. Y. Wang and A. Schönhals, Dielectric and Flash DSC Investigations on an Epoxy Based Nanocomposite System with MgAl Layered Double Hydroxide as Nanofiller, *Thermochim. Acta*, 2019, **677**, 151–161, DOI: [10.1016/j.tca.2019.01.010](https://doi.org/10.1016/j.tca.2019.01.010).
- 38 C. S. Harris and T. G. Rukavina, Lithium Ion Conductors and Proton Conductors: Effects of Plasticizers and Hydration, *Electrochim. Acta*, 1995, **40**(13–14), 2315–2320, DOI: [10.1016/0013-4686\(95\)00185-H](https://doi.org/10.1016/0013-4686(95)00185-H).
- 39 M. Marcinek, A. Bac, P. Lipka, A. Zalewska, G. Żukowska, R. Borkowska and W. Wieczorek, Effect of Filler Surface Group on Ionic Interactions in PEG-LiClO<sub>4</sub>-Al<sub>2</sub>O<sub>3</sub> Composite Polyether Electrolytes, *J. Phys. Chem. B*, 2000, **104**(47), 11088–11093, DOI: [10.1021/jp0021493](https://doi.org/10.1021/jp0021493).
- 40 H. Tanaka, S. Ohshima, S. Ichiba and H. Negita, The Kinetic Deuterium Isotope Effect in the Thermal Dehydration of Boric Acid, *Thermochim. Acta*, 1981, **44**(1), 37–42, DOI: [10.1016/0040-6031\(81\)80269-9](https://doi.org/10.1016/0040-6031(81)80269-9).
- 41 R. Koike, K. Higashi, N. Liu, W. Limwikrant, K. Yamamoto and K. Moribe, Structural Determination of a Novel Polymorph of Sulfathiazole-Oxalic Acid Complex in Powder Form by Solid-State NMR Spectroscopy on the Basis of Crystallographic Structure of Another Polymorph, *Cryst. Growth Des.*, 2014, **14**(9), 4510–4518, DOI: [10.1021/cg5005903](https://doi.org/10.1021/cg5005903).
- 42 M. Amereller, M. Multerer, C. Schreiner, J. Lodermeier, A. Schmid, J. Barthel and H. J. Gores, Investigation of the Hydrolysis of Lithium Bis[1,2-Oxalato(2-)0,0] Borate (LiBOB) in Water and Acetonitrile by Conductivity and NMR Measurements in Comparison to Some Other Borates, *J. Chem. Eng. Data*, 2009, **54**(2), 468–471, DOI: [10.1021/je800473h](https://doi.org/10.1021/je800473h).
- 43 I. S. Noor, S. R. Majid and A. K. Arof, Poly(Vinyl Alcohol)-LiBOB Complexes for Lithium-Air Cells, *Electrochim. Acta*, 2013, **102**, 149–160, DOI: [10.1016/j.electacta.2013.04.010](https://doi.org/10.1016/j.electacta.2013.04.010).
- 44 I. D. E. Villepin, A. Novak and D. Bougeard, A-And B-Phases Of Oxalic Acid, H<sub>2</sub>C<sub>2</sub>O<sub>4</sub>: Vibrational Spectra, Normagcqor-dinate Calculations, And Intrrimqlecul~R Forces, *Chem. Phys.*, 1982, **73**, 291–312.
- 45 S. Lascaud, M. Perrier, A. Vallée, S. Besner, J. Prud'homme and M. Armand, Phase Diagrams and Conductivity Behavior of Poly(Ethylene Oxide)-Molten Salt Rubbery Electrolytes, *Macromolecules*, 1994, **27**(25), 7469–7477, DOI: [10.1021/ma00103a034](https://doi.org/10.1021/ma00103a034).
- 46 B. Sun, J. Mindemark, E. V. Morozov, L. T. Costa, M. Bergman, P. Johansson, Y. Fang, I. Furó and D. Brandell, Ion Transport in Polycarbonate Based Solid Polymer Electrolytes: Experimental and Computational Investigations, *Phys. Chem. Chem. Phys.*, 2016, **18**(14), 9504–9513, DOI: [10.1039/c6cp00757k](https://doi.org/10.1039/c6cp00757k).
- 47 P. G. Bruce and C. A. Vincent, Polymer Electrolytes, *J. Chem. Soc., Faraday Trans.*, 1993, **89**(17), 3187, DOI: [10.1039/ft9938903187](https://doi.org/10.1039/ft9938903187).
- 48 B. J. Sung, P. N. Didwal, R. Verma, A. G. Nguyen, D. R. Chang and C. J. Park, Composite Solid Electrolyte Comprising Poly(Propylene Carbonate) and Li<sub>1.5</sub>Al<sub>0.5</sub>Ge<sub>1.5</sub>(PO<sub>4</sub>)<sub>3</sub> for Long-Life All-Solid-State Li-Ion Batteries, *Electrochim. Acta*, 2021, **392**, 139007, DOI: [10.1016/j.electacta.2021.139007](https://doi.org/10.1016/j.electacta.2021.139007).
- 49 M. Rohde, Y. Cui, C. Ziebert and H. J. Seifert, Thermophysical Properties of Lithium Aluminum Germanium Phosphate with Different Compositions, *Int. J. Thermophys.*, 2020, **41**(3), 1–13, DOI: [10.1007/s10765-020-2607-0](https://doi.org/10.1007/s10765-020-2607-0).
- 50 D. Devaux, R. Bouchet, D. Glé and R. Denoyel, Mechanism of Ion Transport in PEO/LiTFSI Complexes: Effect of Temperature, Molecular Weight and End Groups, *Solid State Ionics*, 2012, **227**, 119–127, DOI: [10.1016/j.ssi.2012.09.020](https://doi.org/10.1016/j.ssi.2012.09.020).
- 51 L. Caradant, N. Verdier, G. Foran, D. Lepage, A. Prébé, D. Aymé-Perrot and M. Dollé, Extrusion of Polymer Blend Electrolytes for Solid-State Lithium Batteries: A Study of Polar Functional Groups, *ACS Appl. Polym. Mater.*, 2021, **3**, 6694–6704, DOI: [10.1021/acsapm.1c01466](https://doi.org/10.1021/acsapm.1c01466).
- 52 I. W. Cheung, K. B. Chin, E. R. Greene, M. C. Smart, S. Abbrent, S. G. Greenbaum, G. K. S. Prakash and S. Surampudi, Electrochemical and Solid State NMR Characterization of Composite PEO-Based Polymer Electrolytes, *Electrochim. Acta*, 2003, **48**(14–16 SPEC.), 2149–2156, DOI: [10.1016/S0013-4686\(03\)00198-1](https://doi.org/10.1016/S0013-4686(03)00198-1).
- 53 P. Müller, C. Szczyka, C. Tsai, S. Schöner, A. Windmüller, S. Yu, D. Steinle, H. Tempel, D. Bresser, H. Kungl and R.-A. Eichel, Capacity Degradation of Zero-Excess All-Solid-



State Li Metal Batteries Using a Poly(Ethylene Oxide) Based Solid Electrolyte, *ACS Appl. Mater. Interfaces*, 2024, **16**(25), 32209–32219, DOI: [10.1021/acsami.4c03387](https://doi.org/10.1021/acsami.4c03387).

54 R. K. Harris, *Nuclear Magnetic Resonance Spectroscopy*, Pitman Publishing INC, Marshfield, Massachusetts, 1983.

55 G. Foran, N. Verdier, D. Lepage, C. Malveau, N. Dupré and M. Dollé, Use of Solid-State NMR Spectroscopy for the Characterization of Molecular Structure and Dynamics in Solid Polymer and Hybrid Electrolytes, *Polymer*, 2021, **13**(8), 1207, DOI: [10.3390/polym13081207](https://doi.org/10.3390/polym13081207).

56 S. Choudhury, Z. Tu, A. Nijamudheen, M. J. Zachman, S. Stalin, Y. Deng, Q. Zhao, D. Vu, L. F. Kourkoutis, J. L. Mendoza-Cortes and L. A. Archer, Stabilizing Polymer Electrolytes in High-Voltage Lithium Batteries, *Nat. Commun.*, 2019, **10**(1), 1–11, DOI: [10.1038/s41467-019-11015-0](https://doi.org/10.1038/s41467-019-11015-0).

57 Y. Benabed, M. Rioux, S. Rousselot, G. Hautier and M. Dollé, Assessing the Electrochemical Stability Window of NASICON-Type Solid Electrolytes, *Front. Energy Res.*, 2021, **9**(230), DOI: [10.3389/fenrg.2021.682008](https://doi.org/10.3389/fenrg.2021.682008).

58 F. Huttner, W. Haselrieder and A. Kwade, The Influence of Different Post-Drying Procedures on Remaining Water Content and Physical and Electrochemical Properties of Lithium-Ion Batteries, *Energy Technol.*, 2020, **8**(2), 1900245, DOI: [10.1002/ente.201900245](https://doi.org/10.1002/ente.201900245).

